W-25-10

Society of Automotive Engineers, Inc.
400 COMMONWEALTH DRIVE, WARRENDALE, PA. 15096

# AEROSPACE INFORMATION REPORT

AIR 1327

Issued 1-15-76
Revised

## ACOUSTIC EFFECTS PRODUCED BY A REFLECTING PLANE



### Table of Contents

Table of Contents (Concluded)





PREPARED BY

SAE COMMITTEE A-21, AIRCRAFT NOISE MEASUREMENT

## LIST OF FIGURES

## LIST OF FIGURES (Concluded)

## 1. INTRODUCTION

The propagation of noise between a source and receiver close to the ground is affected by a number of phenomena. These propagation effects are extremely important in the evaluation of aircraft engine noise in two areas: first, in evaluating the change in acoustic characteristics produced by a source configuration change, and second, in extrapolating measured data to distances remote from the original measurement point.

An extensive body of literature has resulted from investigations of noise propagation phenomena. The Bibliography in Section 9 contains many of these reports, particularly those related to ground plane interference. These propagation effects include atmospheric attentuation of sound, scattering of noise in a turbulent atmosphere, refraction of noise due to wind and temperature gradients, scattering by the ground plane surface, and reflection/absorption by the ground. This latter phenomenon is the subject of this AIR. The basic analysis is straightforward for the ideal case of an infinitely hard surface, a point source of broadband noise, and a stable homogeneous medium.

The purposes of this AIR are to provide technical background associated with the problem of correcting measured noise spectra to the "free field" wherein the measurements are taken in the proximity of a ground plane; to provide practical examples of correction methods; and to present some techniques for minimizing the errors associated with the measurement of noise in the presence of ground planes. The application of this AIR should assist the acoustician in understanding the spectral effects of the reflection phenomena and suggests some methods for obtaining more accurate "free field" acoustic data; however, the AIR does not purport to provide unique, exact solutions to all measurement problems, for each measurement situtation is unique in itself. Of paramount importance to the correction procedures is a good knowledge of the acoustic impedance of the ground plane and the geometry associated with the measurement setup. A method of measuring these ground plane characteristics is described in Section 4.2.2.

Section 5.2 presents a brief discussion of reflection effects in flight noise measurement, and provides some recommendations for ground test techniques aimed toward improving the ability to predict inflight noise.

Section 6 of this AIR provides an insight into the limitations of the current state-of-the-art of measurements and corrections as they pertain to this AIR, and in addition provides recommendations as to additional work that might be carried out to further improve the methods outlined in this AIR.

## 2. THEORETICAL ANALYSIS (POINT SOURCE)

### 2.1 MODEL

The following theoretical bases are taken from analyses made by various authors (References 1,2,3).

The setting up of fundamental relations is based on the following general assumptions:

- The source of sound is assumed to be a point source which produces a stationary and random noise, consistent with the ergodic assumption.
- The microphone lies in the far field of the source for all frequencies.
- In the analyses, atmospheric absorption is ignored since the difference between direct and reflected sound path lengths is generally small compared to the total lengths. This means that it can be assumed that sound pressure level obeys the inverse square law of decay.
- The atmosphere is assumed to be still, isothermal and homogeneous.
- Ground surface irregularities are assumed to be small when compared with the wavelength of the sound in the frequency range of interest, such that specular reflection can be assumed and that the concept of an image source can be adopted.

In the presence of a surface, the recorded noise spectra of a source will be modified by interferences between the direct and reflected sound waves.

The problem is geometrically outlined on Figure (2-1).

### 2.2 ANALYSIS FOR A POINT SOURCE OVER A HARD REFLECTING SURFACE

If the ground is a perfect reflector, the ratio of the resulting mean square pressure to the mean square pressure which would have been measured in the free field is given by (Reference 1,3):

$$R = 1 + \frac{1}{Z^2} + \frac{2}{Z} C\tau \qquad (2.1)$$

where:

$$Z = \frac{r'}{r} \quad : \text{geometrical parameter} \qquad (2.2)$$

$r$ : LENGTH OF THE DIRECT SOUND RAY

$r'$ : LENGTH OF THE REFLECTED SOUND RAY

$r_1$ : PROJECTION OF THE DIRECT RAY ON THE GROUND

$h$ : HEIGHT OF SOURCE ABOVE THE GROUND

$h'$ : HEIGHT OF THE MICROPHONE ABOVE THE GROUND

$Z = \frac{r'}{r}$ : GEOMETRICAL PARAMETER

$\Delta r = r' - r$ : DIFFERENCE BETWEEN REFLECTED AND DIRECT PATH LENGTHS



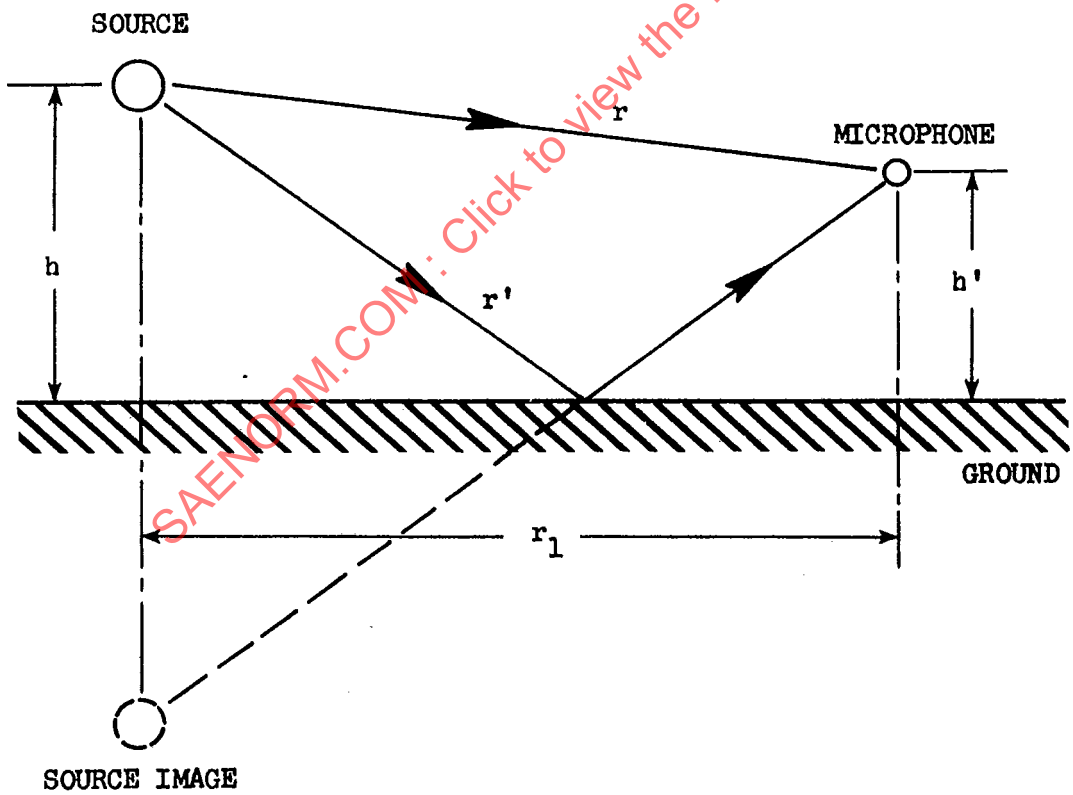


FIGURE (2-1) GEOMETRY OF SOURCE AND RECEIVER WITH RESPECT TO GROUND SURFACE

and

$$C_\tau = \frac{\int_{f_a}^{f_b} w(f) \cos 2\pi \tau f \, df}{\int_{f_a}^{f_b} w(f) \, df} \qquad (2.3)$$

$C_\tau$ is the autocorrelation coefficient of the noise signal in the frequency band ($f_a$, $f_b$) varying with the spectral density w(f) of the direct signal and with the time lag $\tau = \frac{\Delta r}{c} = \frac{r'-r}{c}$ resulting from the path length difference between the direct wave and the reflected wave (c is the ambient speed of sound).

The path length difference, $\Delta r$, is expressed by:

$$\Delta r = \sqrt{r_1^2 + (h + h')^2} - \sqrt{r_1^2 + (h - h')^2} \qquad (2.4)$$

For h and h' small as compared with $r_1$:

$$\Delta r \approx \frac{2 h h'}{r_1} \qquad (2.5)$$

In the particular case of a white noise:

$$w(f) = \text{constant} = w_o$$

and

$$C_\tau = \frac{\sin \pi\tau (f_b - f_a)}{\pi \tau (f_b - f_a)} \cos \pi \tau (f_b + f_a) \qquad (2.6)$$

$f_a$ and $f_b$ being the lower and upper cutoff frequencies associated with the frequency band.

The reflection index associated with this frequency band is expressed in dB, and represents the difference between the total sound level (direct + reflected) and the direct signal alone:

$$\Delta N = 10 \log_{10} R \qquad (2.7)$$

2.2.1 Effect of Bandwidth (ideal filtering)

Pure Tones

In the case of a pure tone, $f_a = f_b = f$ and expression (2.6) becomes

$$C_\tau = \text{Cos } 2\pi \tau f = \text{Cos } 2\pi \frac{\Delta r}{\lambda} \qquad (2.8)$$

so that

$$\Delta N = 10 \text{ Log}_{10} \left[ 1 + \frac{1}{Z^2} + \frac{2}{Z} \text{ Cos } 2\pi \frac{\Delta r}{\lambda} \right] \qquad (2.9)$$

Figure (2-2) shows these reflection indices, as a function of $\Delta r/\lambda$, for different values of the geometrical parameter $Z = r'/r$.

Constant Bandwidth Analysis (white noise)

Expression (2.6) becomes in this case:

$$C_\tau = \frac{\text{Sin } (\pi \frac{\Delta r}{c} \Delta f)}{\pi \frac{\Delta r}{c} \Delta f} \cos (2\pi \frac{\Delta r}{\lambda_i}) \qquad (2.10)$$

with

$$\begin{cases} \Delta f = f_b - f_a \\ f_i = \dfrac{f_b + f_a}{2} = \dfrac{c}{\lambda_i} \end{cases} \qquad (2.11)$$

so that

$$\Delta N = 10 \text{ Log}_{10} \left[ 1 + \frac{1}{Z^2} + \frac{2}{Z} \frac{\text{Sin } (\pi \frac{\Delta r}{c} \Delta f)}{(\pi \frac{\Delta r}{c} \Delta f)} \text{ Cos } (2\pi \frac{\Delta r}{\lambda_i}) \right] \qquad (2.12)$$

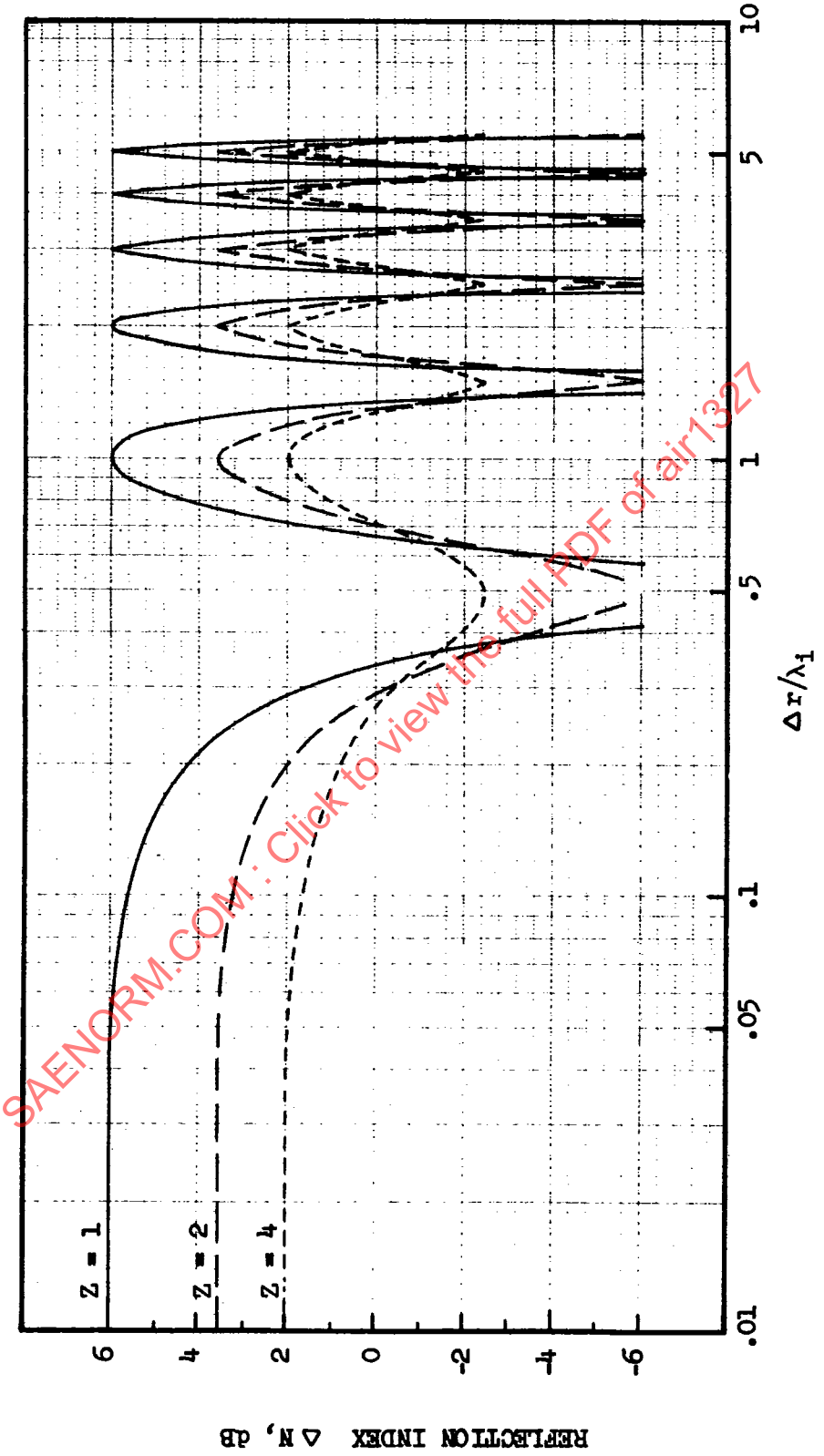


FIGURE (2-2) THEORETICAL REFLECTION INDICES (PURE TONES)
(POINT SOURCE OVER A REFLECTING SURFACE)

Constant-Percentage Bandwidth Analysis (white noise)

In this case, expression (2.6) yields

$$C_\tau = \frac{\mathrm{Sin}(\alpha \frac{\Delta r}{\lambda i})}{(\alpha \frac{\Delta r}{\lambda_i})} \mathrm{Cos}\ (\beta \frac{\Delta r}{\lambda_i}) \qquad (2.13)$$

with

$$\begin{cases} \alpha = 2\pi\ (\frac{\Delta f}{2\ f_i}) \\ \beta = 2\pi \sqrt{1 + (\frac{\Delta f}{2\ f_i})^2} \end{cases} \qquad (2.14)$$

$f_i$ being the geometric mean frequency of filter ($f_i = \sqrt{f_a f_b}$) and $\lambda_i = c/f_i$

For 1/3 octave band analysis: $\frac{\Delta f}{f_i} = 0.231$ and for octave band analysis: $\frac{\Delta f}{f_i} = 0.707$.

The reflection index is:

$$\Delta N = 10\ \mathrm{Log}_{10}\ [1 + \frac{1}{Z^2} + \frac{2}{Z} \frac{\mathrm{Sin}\ (\alpha \frac{\Delta r}{\lambda_i})}{(\alpha \frac{\Delta r}{\lambda_i})} \cos\ (\beta \frac{\Delta r}{\lambda_i})] \qquad (2.15)$$

Figures (2-3) and (2-4) represent this expression, as a function of $\Delta r/\lambda_i$, respectively for 1/3 octave and octave analysis.

2.2.2 Effect of Source and Receiver Height Variations

Variations in height are completely described by the value of the geometrical parameter Z which is a measure of the attenuation of the reflected wave, as compared to the direct wave, in accordance with the inverse-square law of decay.

For most practical cases of far field measurements or predictions, Z, which is expressed by

$$Z = 1 + \frac{\Delta r}{r}$$

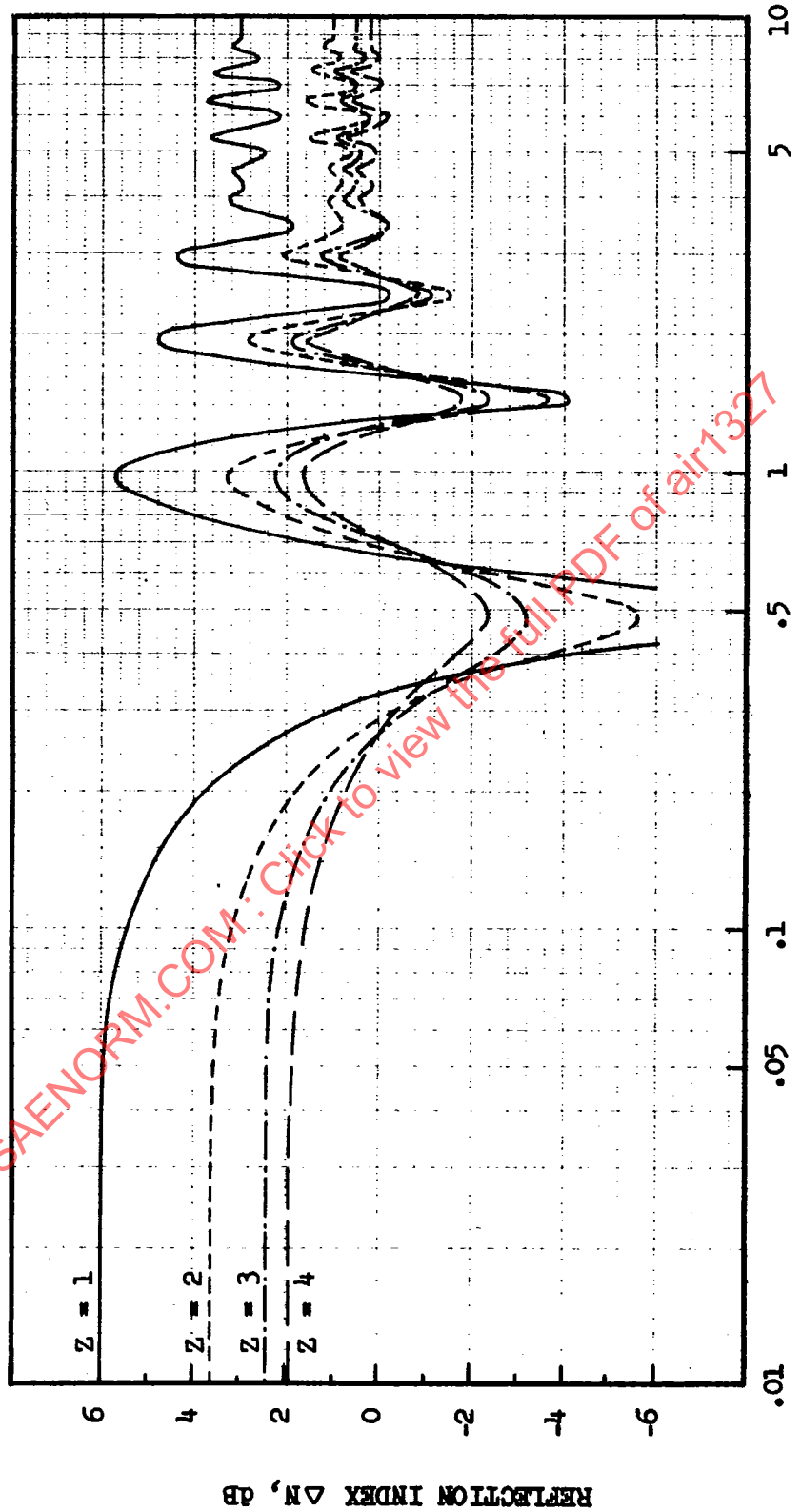


FIGURE (2-3) THEORETICAL REFLECTION INDICES (1/3 OCTAVE BANDS)
(POINT SOURCE OVER A REFLECTING SURFACE)

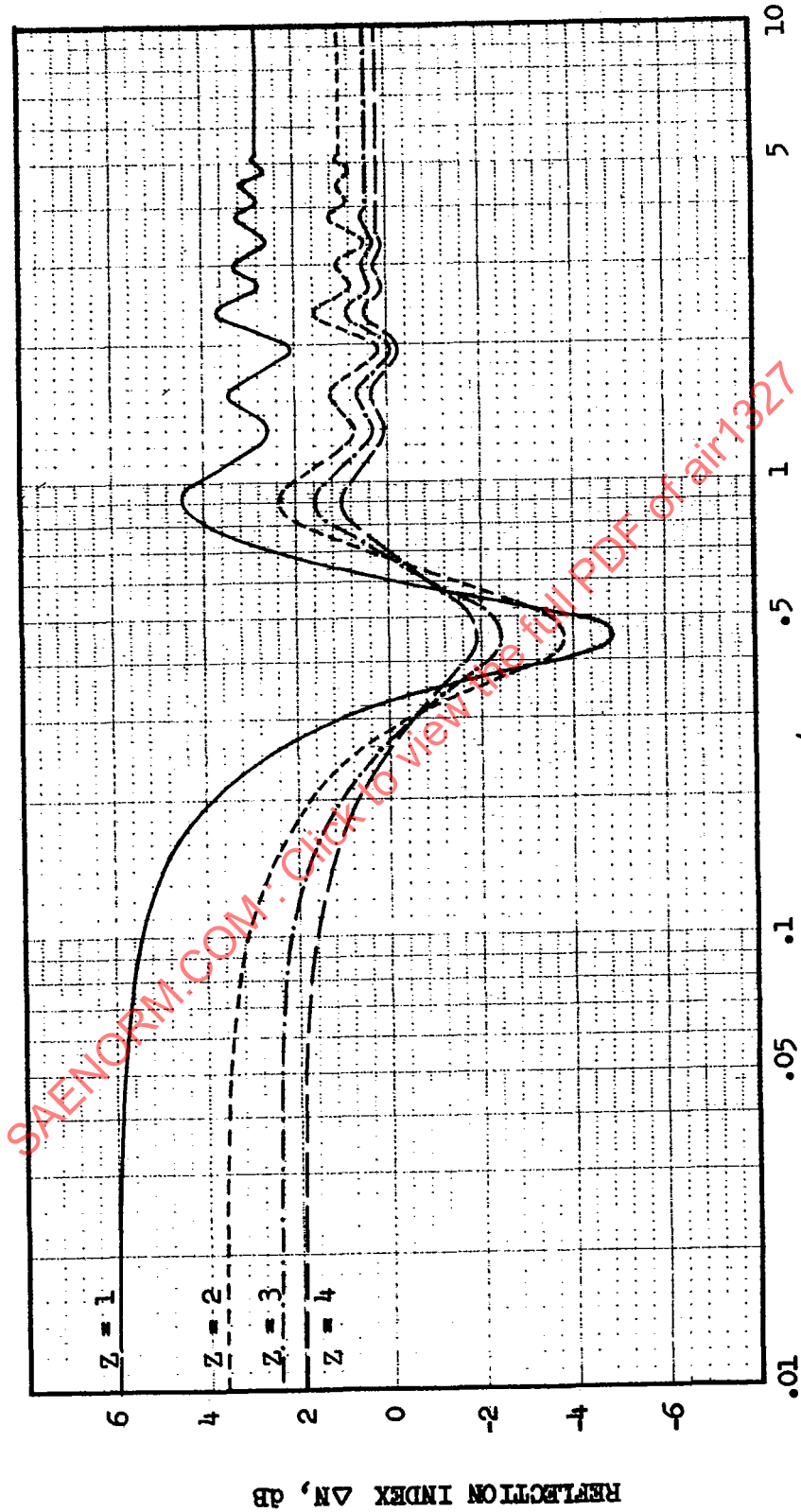


FIGURE (2-4) THEORETICAL REFLECTION INDICES (OCTAVE BANDS)
(POINT SOURCE OVER A REFLECTING SURFACE)

can be assumed to be close to unity because in these cases, $\Delta r$, which is of the order of magnitude of the wavelengths of interest, is generally small compared to r.

For high values of Z (that means for example high values of h and h' compared with r) the interference patterns become negligible. For instance, the reflection indices are smaller than 1 dB ($\Delta N \leq |1|$) if $Z \geq 8$. Unfortunately, such high values of Z, which can be reached on model test facilities, are unfeasible on engine test rigs or for inflight measurements because they would need impractical microphone heights.

If h or h' is zero (the receiver or the source are flush with the ground surface), we have a limiting case of nearly totally constructive interference, and pressure doubling results at all frequencies, giving a reflection index of +6 dB.



### 2.2.3 Effects of Spectrum Density Slope

A systematic study of the influence of the spectrum density slope has shown (Reference 4) that if, in the frequency band under consideration, the spectrum density w(f) can be written:

$$w(f) = k\, f^n$$

and if $|n| \leq 2$ (as in the case of pink noise, where n = -1), data given for white noise in Section 2.2.1. can be applied without error to 1/3 octave band analysis and with negligible error to octave band analysis of these spectra. In fact, the same data remain valid for slopes of $|n| \leq 3$ with a fair approximation (error smaller than 0.5 dB for 1/3 octave analysis and smaller than 1 dB for octave analysis).

## 2.3 ANALYSIS FOR A POINT SOURCE OVER A FINITE IMPEDANCE SURFACE

If the ground is partially absorbing, the surface is assumed to be locally reacting, i.e.: its normal acoustic impedance $Z_n$ is independent of the configuration of the incident wave.

In order to simplify the analysis, we will assume that the sound wave, in the vicinity of the theoretical reflection point, can be considered a plane wave because its radius of curvature is of the order of magnitude of the source-receiver distance.

For a given angle of incidence $\theta$, the complex plane wave reflection coefficient for amplitude will vary with frequency and is expressed by:

$$Q = \frac{Z_n \text{ Cos } \theta - \rho C}{Z_n \text{ Cos } \theta + \rho C} = |Q| e^{j\delta} \qquad (2.16)$$

$\rho c$ being the characteristic acoustic impedance of the air, $|Q|$ the magnitude of the reflection coefficient and $\delta$ its phase.

The sound field at any point of the half space above the ground surface is then obtained by adding the direct wave from the source to the corresponding wave from the image source, the latter being multiplied by the reflection coefficient.

There are limitations to the applicability of this simple approach to the problem because practically one never has plane waves and the definition of the reflection coefficient no longer holds near grazing incidence ($\theta \simeq 90°$).

Nevertheless, for many practical cases, there is a reasonable agreement between the proposed theoretical approach and data measured over ground such as grassland.

To simplify the problem, the reflection coefficient Q will be assumed to be constant in each of the frequency bands ($f_a$, $f_b$) corresponding to the selected type of analysis and will be given by a value corresponding to the bandwidth center frequency $f_i$:

$$Q_i = |Q_i| e^{j\delta_i} \qquad (2.17)$$

For a given incidence, i.e.: for a given geometry of the problem, $Q_i$ values are usually calculated from values of the normal specific impedance ratio of the surface:

$$\frac{Z_n}{\rho c} = \frac{R_A}{\rho c} + j \frac{X_A}{\rho c} \qquad (2.18)$$

where $R_A/\rho c$ and $X_A/\rho c$ are the acoustic resistance and reactance ratios.

It follows from expressions (2.17) and (2.18) that $|Q_i|$ and $\delta_i$ can be written:

$$|Q_i| = \frac{\sqrt{\left(\left|\frac{Z_n}{\rho c}\right|^2 \cos^2\theta - 1\right)^2 + 4\left(\frac{X_A}{\rho c}\right)^2 \cos^2\theta}}{\left(\left|\frac{Z_n}{\rho c}\right|^2 \cos^2\theta + 1 + 2\frac{R_A}{\rho c}\cos\theta\right)} \qquad (2.19)$$

$$\delta_i = \begin{cases} \sin\delta_i = \dfrac{2\dfrac{X_A}{\rho c}\cos\theta}{\sqrt{\left(\left|\frac{Z_n}{\rho c}\right|^2 \cos^2\theta - 1\right)^2 + 4\left(\frac{X_A}{\rho c}\right)^2 \cos^2\theta}} \\ \cos\delta_i = \dfrac{\left|\frac{Z_n}{\rho c}\right|^2 \cos^2\theta - 1}{\sqrt{\left(\left|\frac{Z_n}{\rho c}\right|^2 \cos^2\theta - 1\right)^2 + 4\left(\frac{X_A}{\rho c}\right)^2 \cos^2\theta}} \end{cases} \qquad (2.20)$$

$X_A$ and $R_A$ being taken for the center frequency of the frequency band under consideration.

In the case of a point source delivering a pure tone the reflection index is given by (References 2, 4):

$$\Delta N = 10\,\mathrm{Log}_{10}\left[1 + \left(\frac{|Q_i|}{Z}\right)^2 + 2\frac{|Q_i|}{Z}\cos\left(2\pi\frac{\Delta r}{\lambda_i} - \delta_i\right)\right] \qquad (2.21)$$

In the case of a white noise and for an ideal constant-percentage bandwidth analysis ($\Delta f/f_i$ = constant), we will have:

$$\Delta N = 10\,\mathrm{Log}_{10}\left[1 + \left(\frac{|Q_i|}{Z}\right)^2 + 2\frac{|Q_i|}{Z}\frac{\sin\left(\alpha\frac{\Delta r}{\lambda_i}\right)}{\left(\alpha\frac{\Delta r}{\lambda_i}\right)}\cos\left(\beta\frac{\Delta r}{\lambda i} - \delta_i\right)\right] \qquad (2.22)$$

It is worthwhile mentioning an alternative to the plane wave analysis given above. Such an analysis can be found, for example, in Item (35) in the Bibliography. More complicated than that of the present approach, this spherical wave analysis does not fail at grazing incidence and the differences between the two are insignificant at angles above grazing. Because of its higher sophistication, the applicability of this method is presently limited to pure tones.

In the presence of an absorbing ground surface, it is obvious that representations of the reflection process, having the same degree of simplicity as those described in Section 2.2 cannot be established. Each case becomes a specific one, depending not only on path length difference, but also on incidence angle and in particular, on the normal acoustic impedance of the ground surface. Therefore, the main problem consists in knowing the acoustic resistance and reactance of the ground surface above which measurements are made or for which noise predictions have to be worked out.

If those characteristics cannot be measured, it is possible to use values of Figure (2-5) taken from the few experimental data published to date (Reference 5). Experimental technique might also be employed to obtain the reflection coefficients of a given ground surface. Such a technique is described briefly in Section 4.2.2.

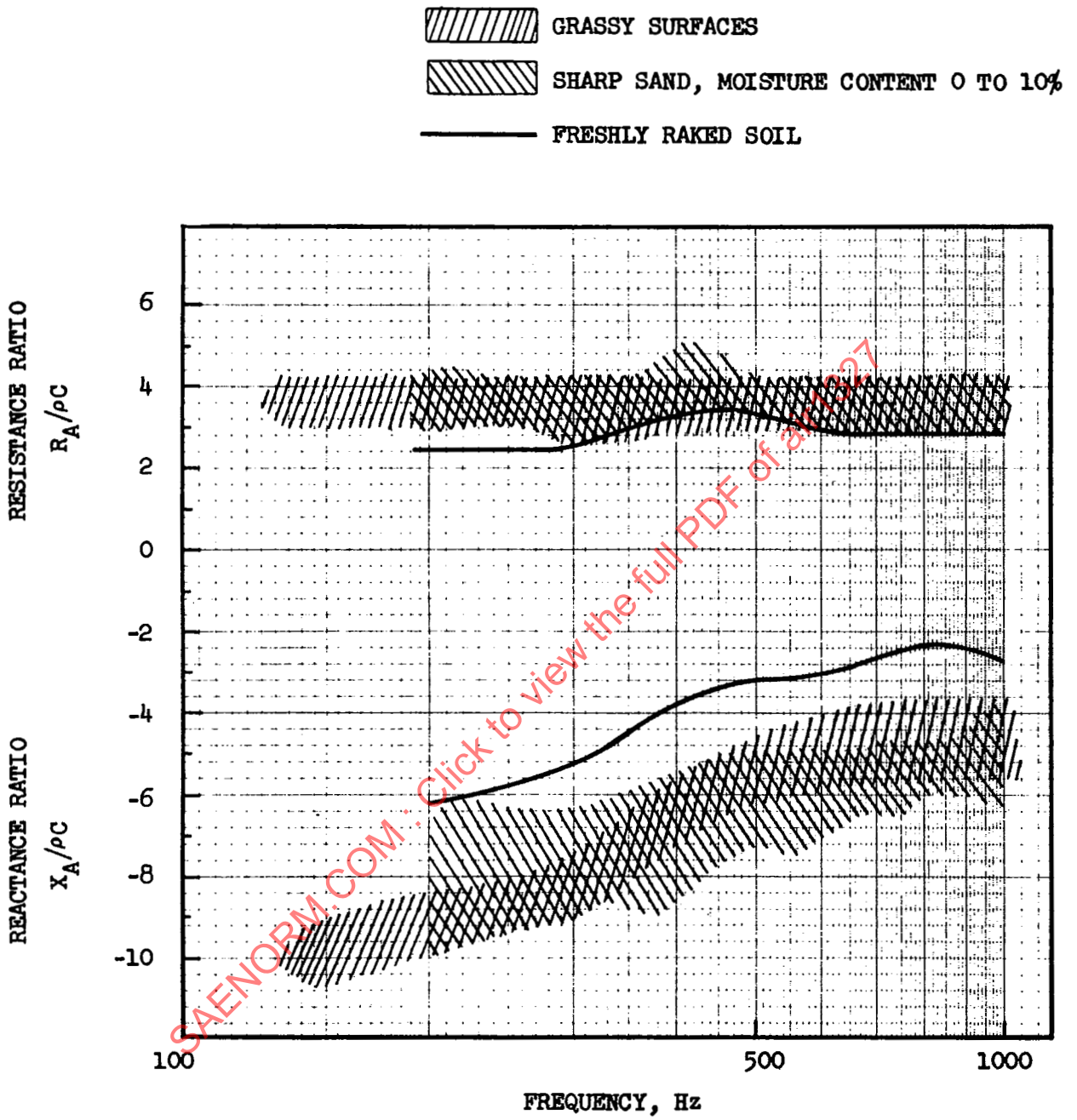




FIGURE (2-5) SOME MEASURED VALUES OF NORMAL IMPEDANCE OF DIFFERENT GROUND SURFACES

## 3. APPLICATION TO BROADBAND NOISE SPECTRA FROM JET ENGINES (Extended Sources)

### 3.1 ANALYSIS

To a first approximation, the noise source constituted by an exhaust jet can be considered as a cylindrical source, defined by the nozzle contour and having a length of up to 10 to 15 nozzle diameters, depending on jet exhaust conditions. It is obvious that for an aircraft in flight, the source-receiver distances are always large compared to these source dimensions and in practice, the source can therefore be considered as a point source. The situation is not so simple for noise measurements around a static engine on the ground. Let us assume first that the jet, which is generally parallel to the ground surface, can be considered as a line source (i.e., all the noise sources of the jet are concentrated on the jet axis). The path length difference $\Delta r_L$ for a source located at an axial distance L from the nozzle center can then be written:

$$\Delta r_L = \sqrt{L^2 + r_1^2 - 2Lr_1 \cos\theta + (h+h')^2} - \sqrt{L^2 + r_1^2 - 2Lr_1 \cos\theta + (h-h')^2} \qquad (3.1)$$

where $r_1$ is the projection on the ground plane of the line joining the nozzle center and the microphone, $\theta$ the angle between the projection on the ground of the jet axis and $r_1$, h and h' respectively the source and receiver heights.

Because noise measurements are generally performed in the far field, i.e., at distances $r_1$ which are at least 50 to 100 nozzle diameters (and consequently several wavelengths corresponding to the lowest frequencies of interest) from the nozzle exit, $r_1$ is large compared to the source dimension L and to h and h'.

In this case, the relative error made by assuming all sources concentrated at the nozzle center is therefore, taking account of relation (2.4):

$$\varepsilon = \frac{\Delta r_L - \Delta r}{\Delta r} \simeq \left(1 + \frac{L^2}{r_1^2} - 2\frac{L}{r_1}\cos\theta\right)^{-\frac{1}{2}} - 1 \qquad (3.2)$$

This error is smallest around $\theta = 90°$ and highest in the vicinity of $\theta = 0°$ and $\theta = 180°$. The highest errors are obtained for the largest values of L. As an example, let us take a typical value of $r_1$ (i.e. $r_1 = 75D$) and calculate for several values of L/D, the error $\varepsilon$ for different values of $\theta$. The results are summarized in the table below:

| | $\theta = 20°$ | $\theta = 90°$ | $\theta = 180°$ |
|---|---|---|---|
| L/D = 10 | $\varepsilon$ = 14% | - 1% | - 12% |
| L/D = 5 | 6.5% | - 2% | - 6% |

If the actual source distribution of a jet were known (f versus L), it would be possible to avoid any error and to calculate the established path length differences corresponding to each source of frequency f (or wavelength $\lambda$) and to establish the corresponding reflection indices. But this distribution has still to be established.

Fortunately, the longest wavelengths are emitted far downstream of the nozzle exit and the shortest close to the nozzle and it is easy to show that for current engine noise test beds, these errors have no direct consequence on the correction procedure, since for the large L/D source position, current $\Delta r/\lambda$ are on the left hand side flat part of the reflection index curves.

For practical purposes, this axial source distribution can therefore be neglected and the whole jet can be considered as a circular distribution of noise around the nozzle lip.

Furthermore, the slopes of the sound pressure spectral density in the noise field of a jet are seldom higher than |3| (see Section 2.2.3) and consequently, a white noise can be assumed for the analysis of jet noise reflection phenomena. In addition, it will be assumed, as in 2.1, that jet noise is a stationary random noise, meeting the ergodic assumption.

3.1.1 Jet at a High Elevation Above the Ground Surface

If the jet is at a high altitude above the ground (say h > 10 D), it can therefore be considered that this circular distribution is equivalent to a point source located at the nozzle center (D is the nozzle diameter for circular nozzles or the equivalent diameter based on area for non-circular nozzles). This is the case for a flying aircraft and for engine noise test facilities in which the engine can be installed at a high elevation (more than 10 nozzle diameters).

Then, relations drawn under 2.2 and 2.3 can be directly applied to the calculation of reflection indices.

3.1.2 Jet Near the Ground Surface

When the jet, which is assumed to be horizontal, is near the ground, it can be shown that the vertical distribution of elementary sources, which are assumed to be located around the nozzle lip, plays a very important role. This distribution leads to a partial damping of peaks and dips of the reflection index curves.

It is assumed that the noise source consists of n independent or incoherent elementary sources. This assumption is valid for a jet in which the distance between elementary sources is higher than the peripheral correlation length. The following independence criterion can be adopted (Reference 4):

$$\ell \geq 0.04 \frac{U}{f} \qquad (3.3)$$

where U is the jet velocity and $\ell$ the distance between two consecutive sources of frequency f.

3.1.2.1 Perfect Reflecting Surface

For these n independent sources, the ratio of the resulting mean square pressure to the free field mean square pressure is expressed as follows (Reference 4):

$$R \simeq 1 + \frac{1}{Z_m^2} + \frac{2}{n Z_m} \sum_{K=1}^{K=n} C_{\tau_k} \qquad (3.4)$$

This formulation leads, in the case of a white noise and for an ideal constant-percentage bandwidth analysis ($\frac{\Delta f}{f_i}$ = Constant), to the reflection index:

$$\Delta N = 10 \, \mathrm{Log}_{10} \left[ 1 + \frac{1}{Z_m^2} + \frac{2}{nZ_m} \sum_{K=1}^{K=n} \frac{\mathrm{Sin} \left( \alpha \frac{\Delta r_k}{\lambda_i} \right)}{\left( \alpha \frac{\Delta r_k}{\lambda_i} \right)} \mathrm{Cos} \left( \beta \frac{\Delta r_k}{\lambda_i} \right) \right] \qquad (3.5)$$

where $Z_m$ is the geometrical parameter corresponding to the nozzle center or, for more precise calculations (Section 3.1), to a point located on the jet axis at a distance L from the nozzle center.

Practically, the jet will be considered as a vertical distribution of n elementary sources, separated from each other by a distance d such that $d/h_m \leq 0.10$ (Reference 4).

Symbols are given by the following figure:

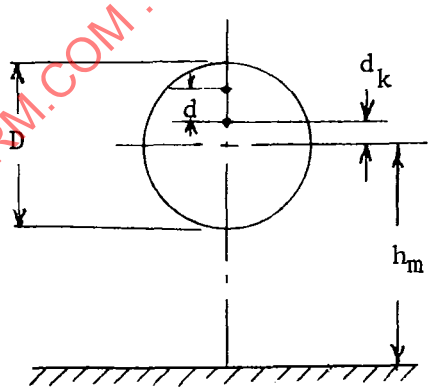


For an elementary source located at a distance $d_k$ from the nozzle center-line (taken as the center of the vertical distribution of n sources), the path length difference is:

$$\frac{\Delta r_k}{\lambda_i} = \frac{\Delta r_m}{\lambda_i} \left(1 + \frac{d_k}{h_m}\right) \qquad (3.6)$$

where $\Delta r_m$ is the path length difference corresponding to the nozzle center or to a point located on the jet axis at a distance L from the nozzle center.

As an example of application of these results, Figures (3-1) and (3-2) show respectively for 1/3 octave and octave band analysis, the reflection index values for a vertical distribution of three sources at three different values of the parameter $D/h_m$. These curves can apply to most practical cases.

Note: Independently from these source distribution effects, it is important that the jet engine height be large enough to avoid asymmetric jet mixing, caused by ground proximity, and, as a consequence, asymmetric directivity characteristics of the jet noise.

3.1.2.2 Finite Impedance Surface

In the case of a jet near a finite impedance surface, assuming that $|Q_i|$ and $\delta_i$ are the same for the n elementary sources (negligible variations of the incidence angle), the reflection index is given by:

$$\Delta N = 10 \operatorname{Log}_{10}\left[1 + \left(\frac{|Q_i|}{Z_m}\right)^2 + 2\frac{|Q_i|}{nZ_m} \sum_{K=1}^{K=n} \frac{\operatorname{Sin}\left(\alpha\frac{\Delta rk}{\lambda i}\right)}{\left(\alpha\frac{\Delta rk}{\lambda_i}\right)} \cos\left(\beta\frac{\Delta rk}{\lambda_i} - \delta_i\right)\right] \qquad (3.7)$$

But in this case, no simple generalized curves, like those of Figures (3-1) and (3-2) can be proposed. For each given problem, the reflection indices have to be calculated, using relation (3.7) together with relations (2.19), (2.20) and (3.6), if the acoustic characteristics of the ground are known. If not, typical impedance values of Figure (2-5) might be used for calculating the complex reflection coefficient, or the experimental technique described in Section 4.2.2 might be used to measure the actual ground impedance of the test area.

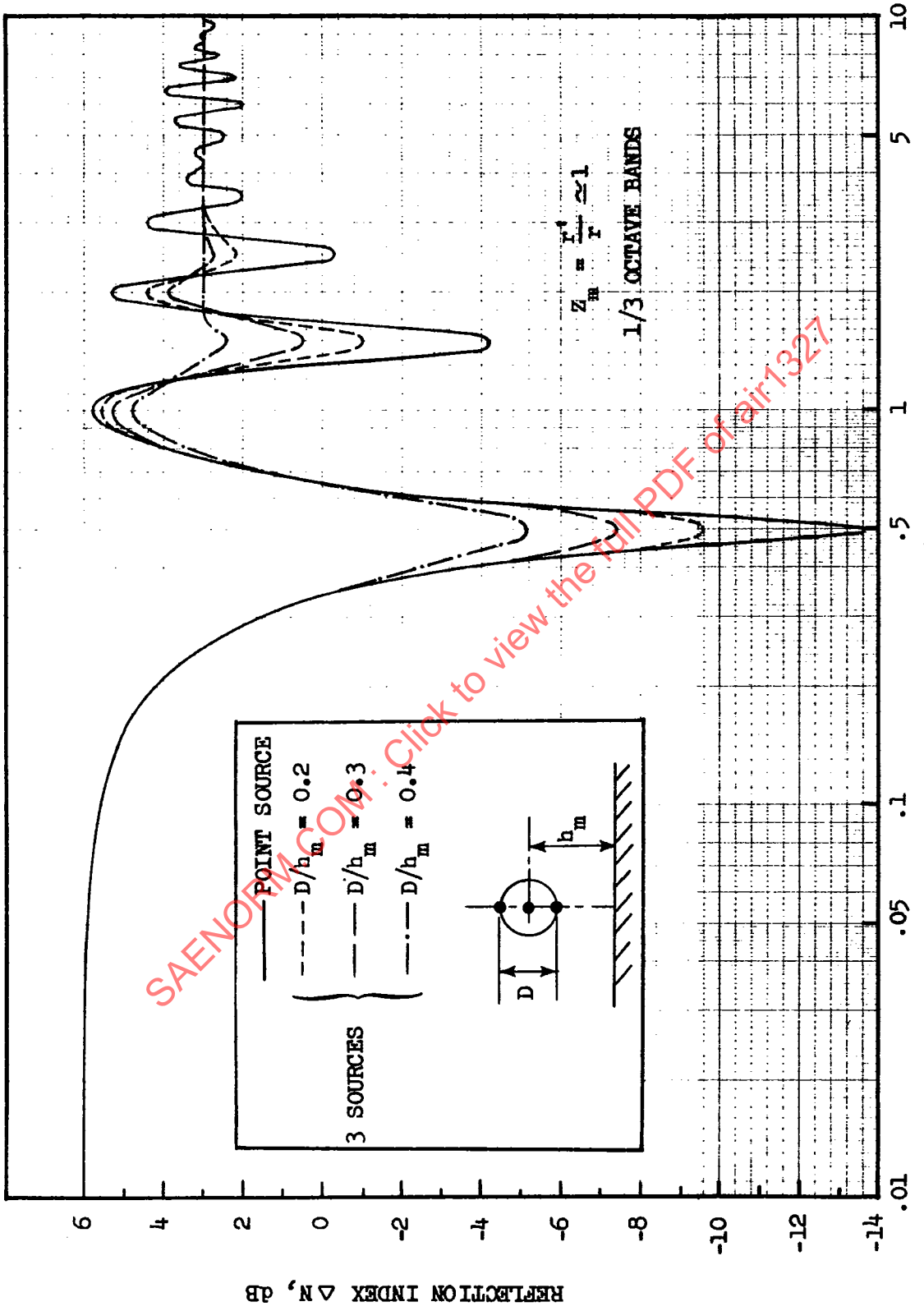


FIGURE (3-1) EFFECT OF PARAMETER $D/h_m$ ON JET REFLECTION INDEX

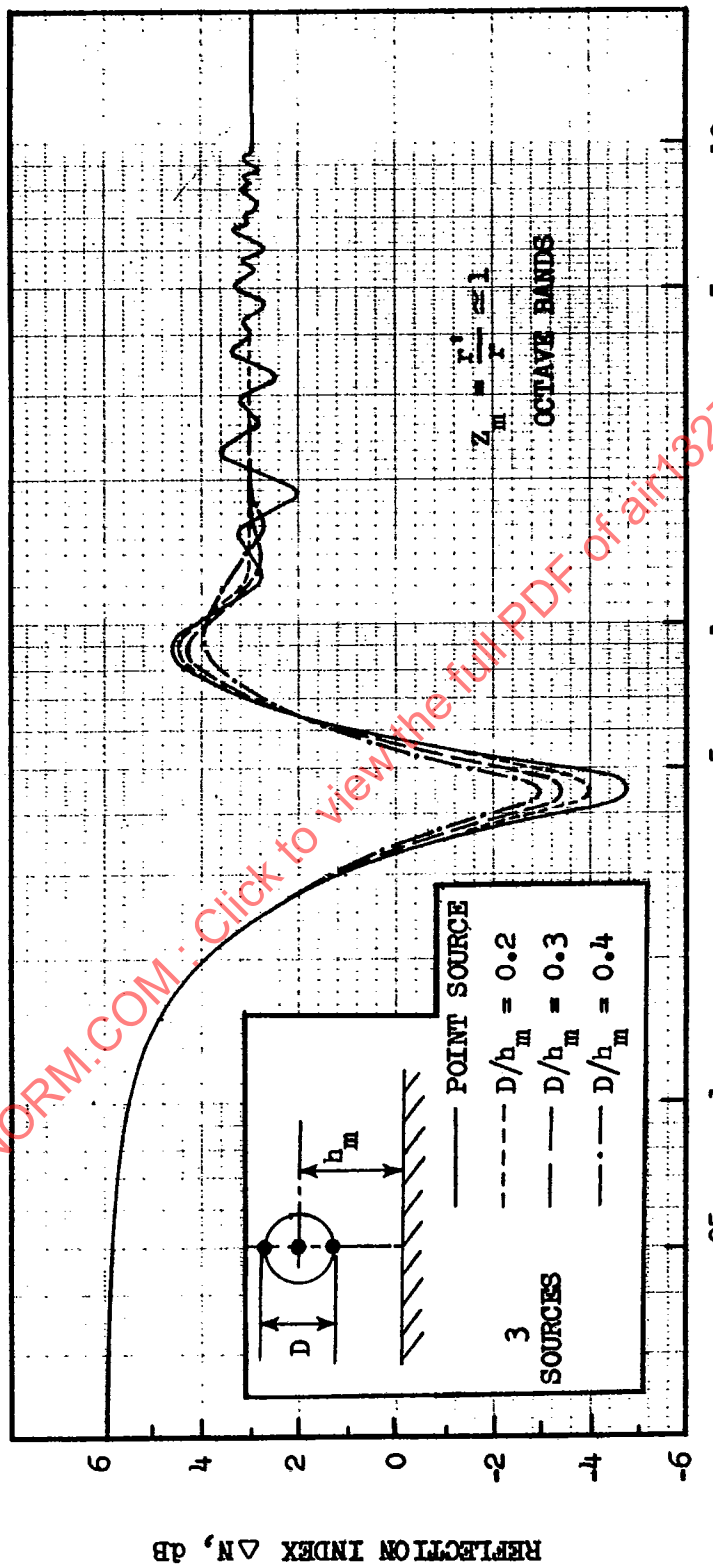


FIGURE (3-2) EFFECT OF PARAMETER $D/h_m$ ON JET REFLECTION INDEX

## 3.2 COMPARISONS WITH EXPERIMENTAL DATA

In order to support the previous theoretical analysis, some comparisons between measured and corrected data are presented.

### 3.2.1 Scale Model Jets

In Figures (3-3) and (3-4) theoretical and measured reflection indices are compared. The measured values were obtained with model jets, in an anechoic chamber, by comparing measured free field jet noise spectra with the corresponding spectra as measured above a fully reflecting surface. Various experimental configurations were used, all corresponding to $D/h_m \leq 0.10$. For both 1/3 octave and octave analysis, a satisfactory agreement between measured and calculated data can be noted.

Figures (3-5) and (3-6) show some model jet noise spectra which have been measured in free field conditions (anechoic chamber) and also over a fully reflecting surface. In both figures, the measured free field spectra have been compared with the free field spectra obtained by applying the theoretical reflection indices of Figure (3-1) for $D/h_m = 0.2$, or relation (3.5), to the spectra which were measured over the reflecting surface.

### 3.2.2 Full Scale Jets

The last two figures illustrate comparisons of engine jet noise spectra measured above a fully reflecting surface (concrete) and above grassland, together with the corresponding calculated free field spectra, obtained by applying the theoretical corrections discussed in the former sections.

Figure (3-7) shows a jet noise spectrum measured above a fully reflecting surface (concrete) and the corresponding calculated free field spectrum obtained by applying corrections calculated with relation (3.5) for a three source distribution or by using Figure (3-1) ($D/h_m = 0.2$).

Figure (3-8) compares a jet noise spectrum measured above grass and the free field spectrum obtained by applying corrections given by relation (2.22), using relations (2.16) to (2.20), and extrapolated data for grassy surfaces derived from Figure (2-5).

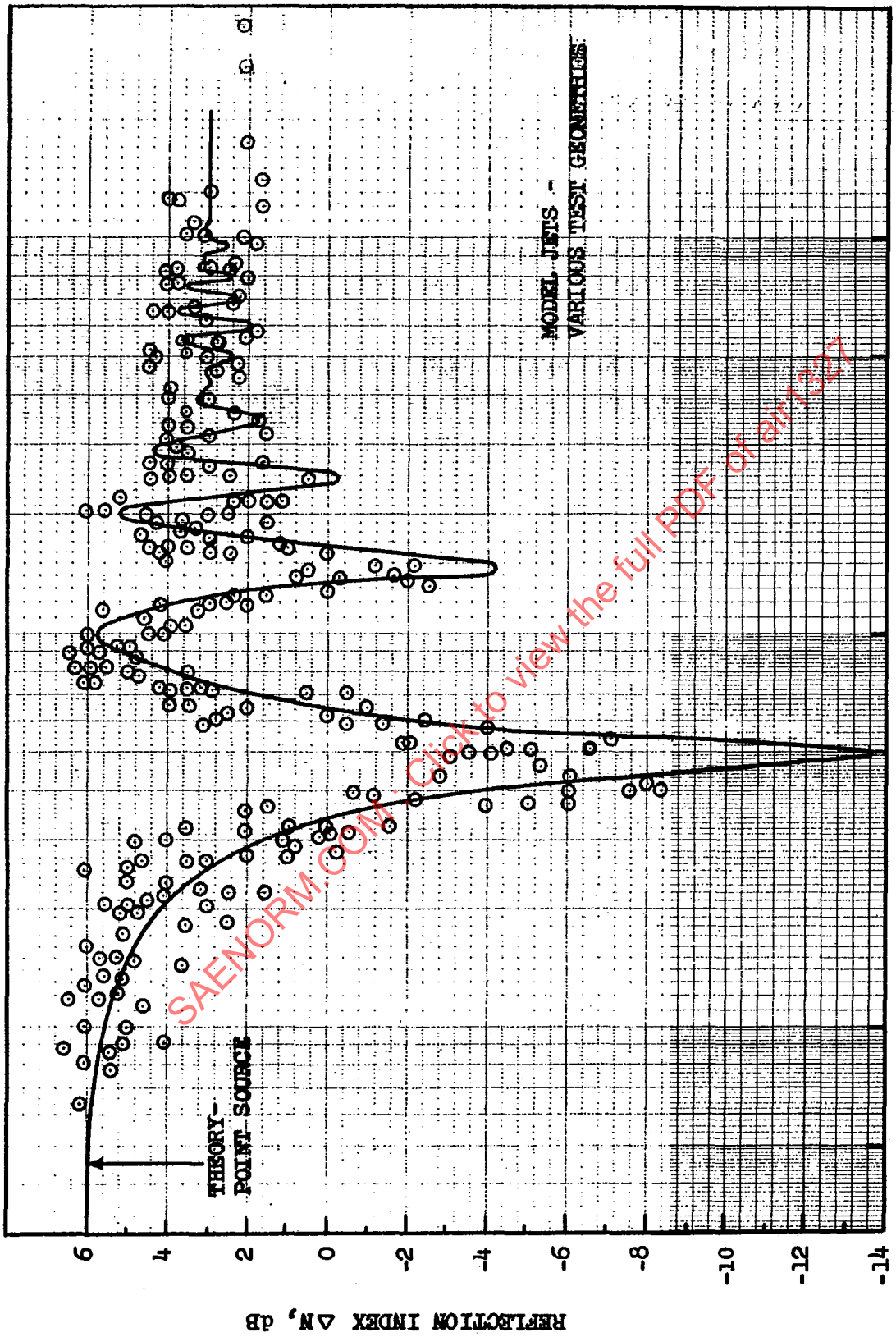


FIGURE (3-3) COMPARISON OF TEST RESULTS WITH THEORY - 1/3 OCTAVE ANALYSIS

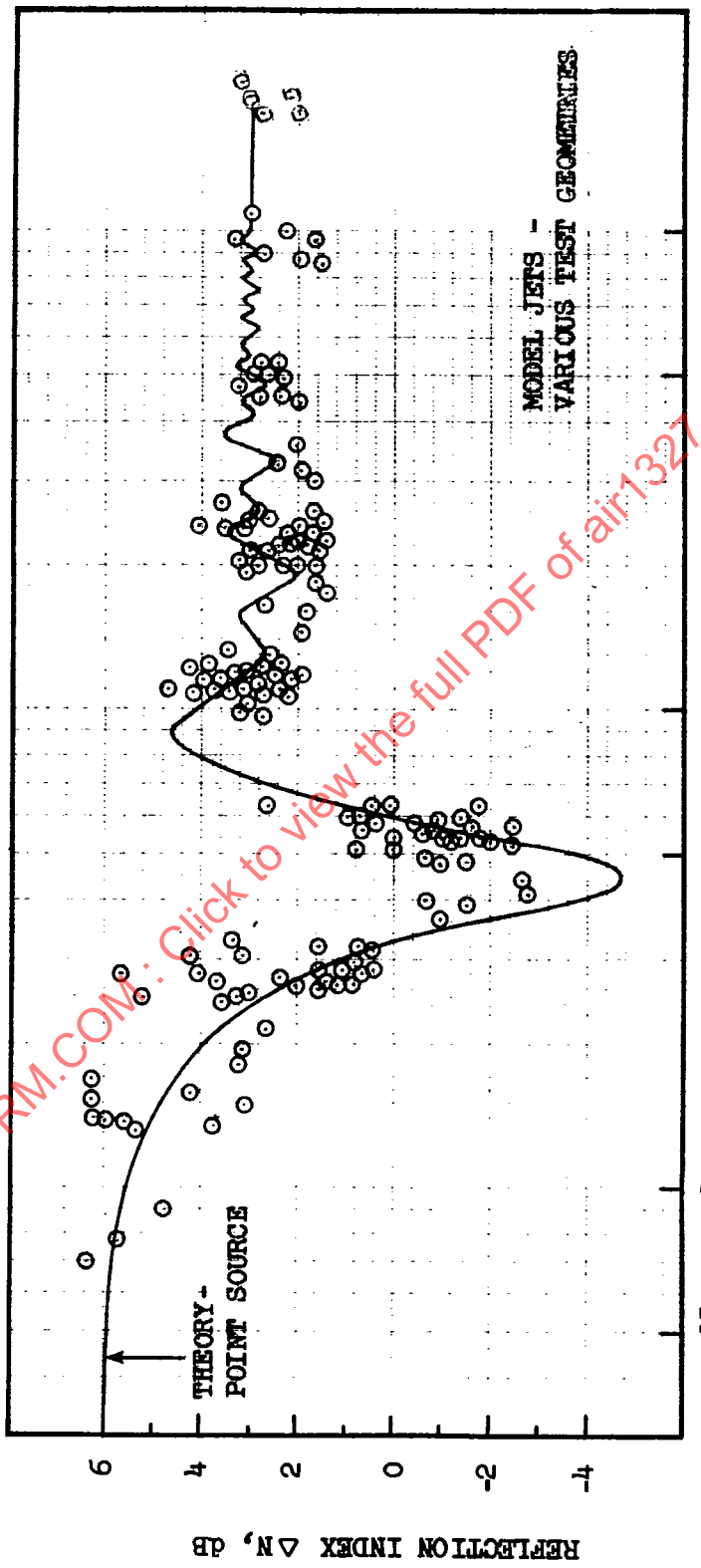


FIGURE (3-4) COMPARISON OF TEST RESULTS WITH THEORY - OCTAVE ANALYSIS

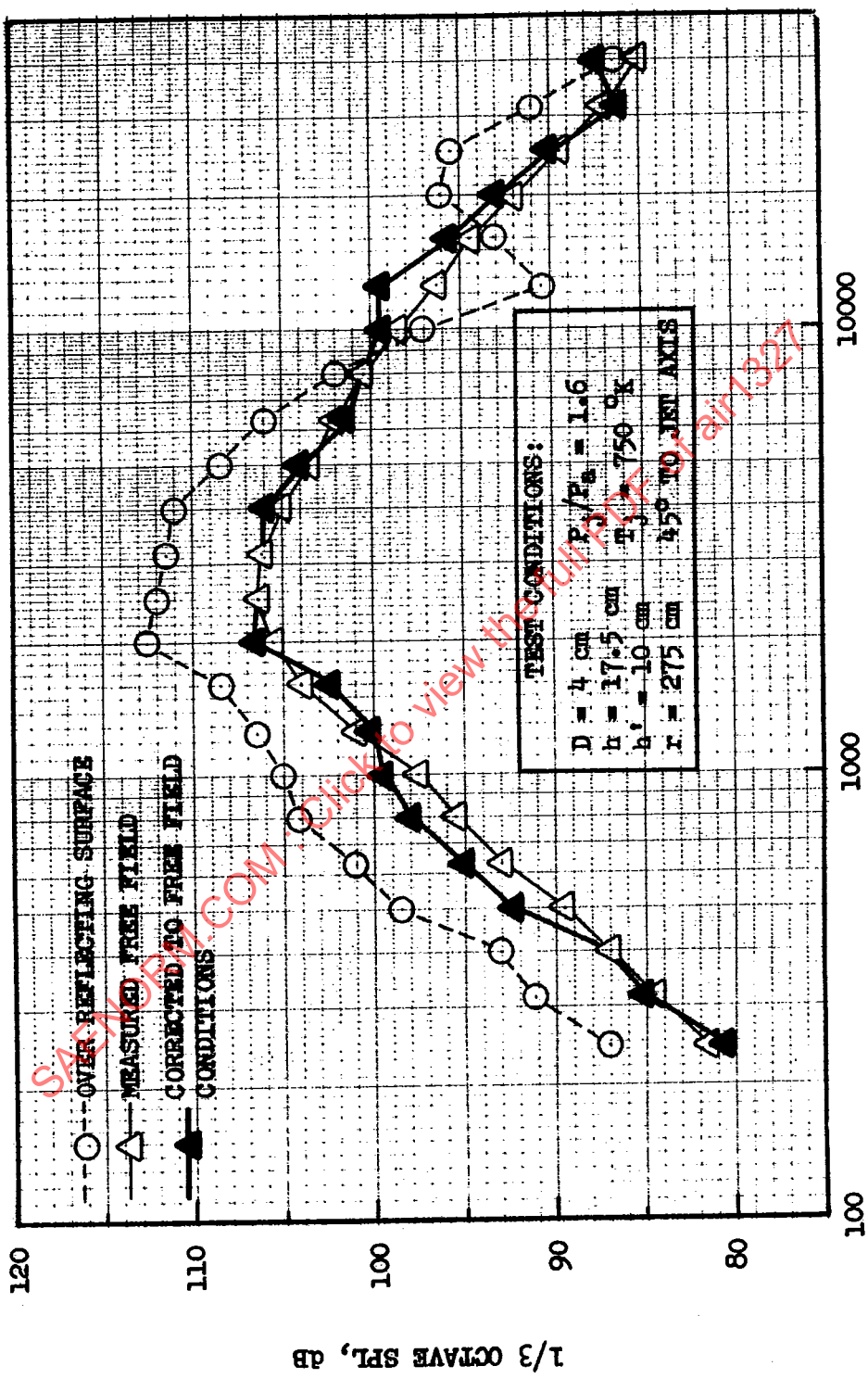


FIGURE (3-5) EXPERIMENTAL RESULTS ON MODEL JETS

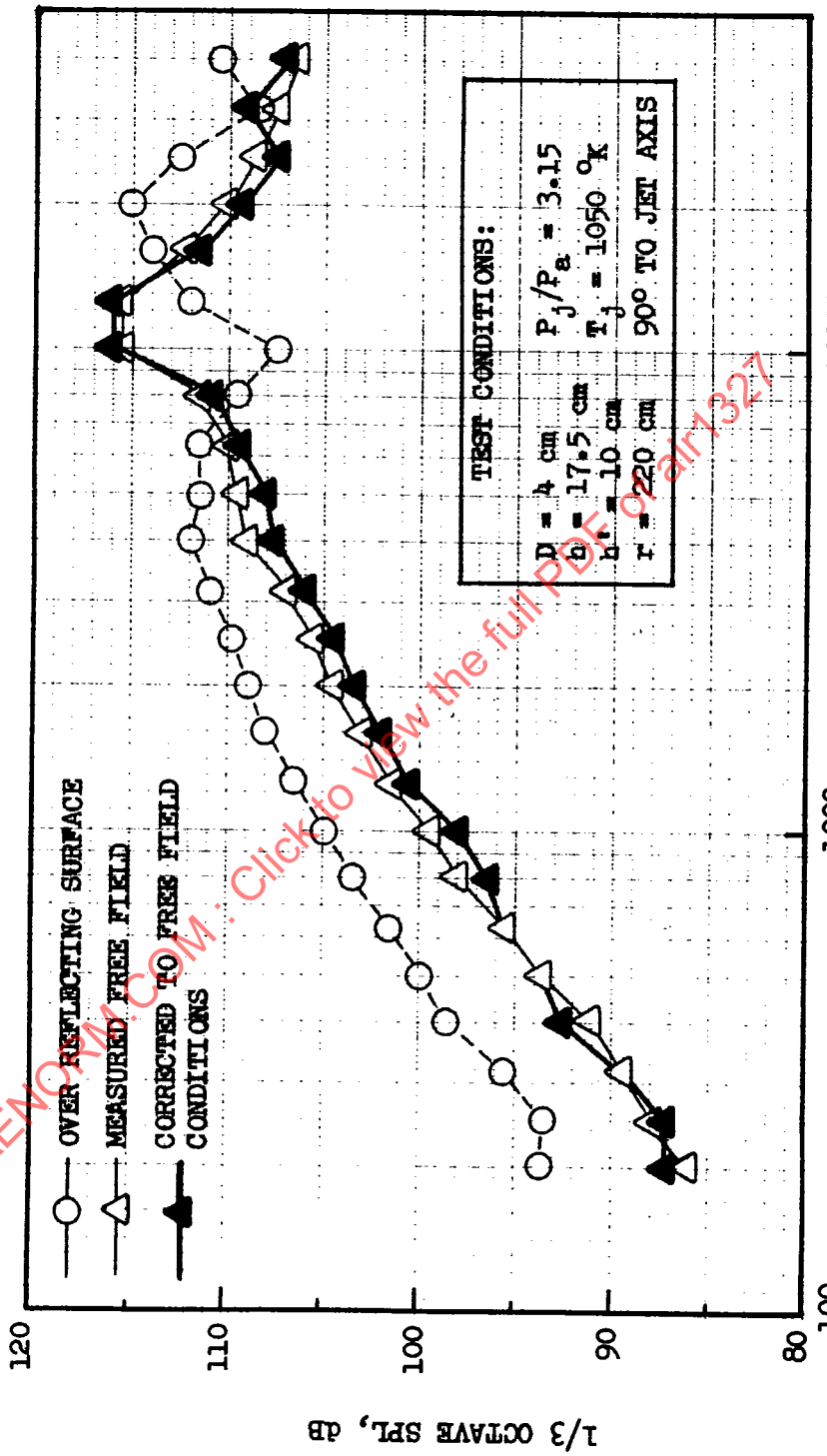


FIGURE (3-6) EXPERIMENTAL RESULTS ON MODEL JETS

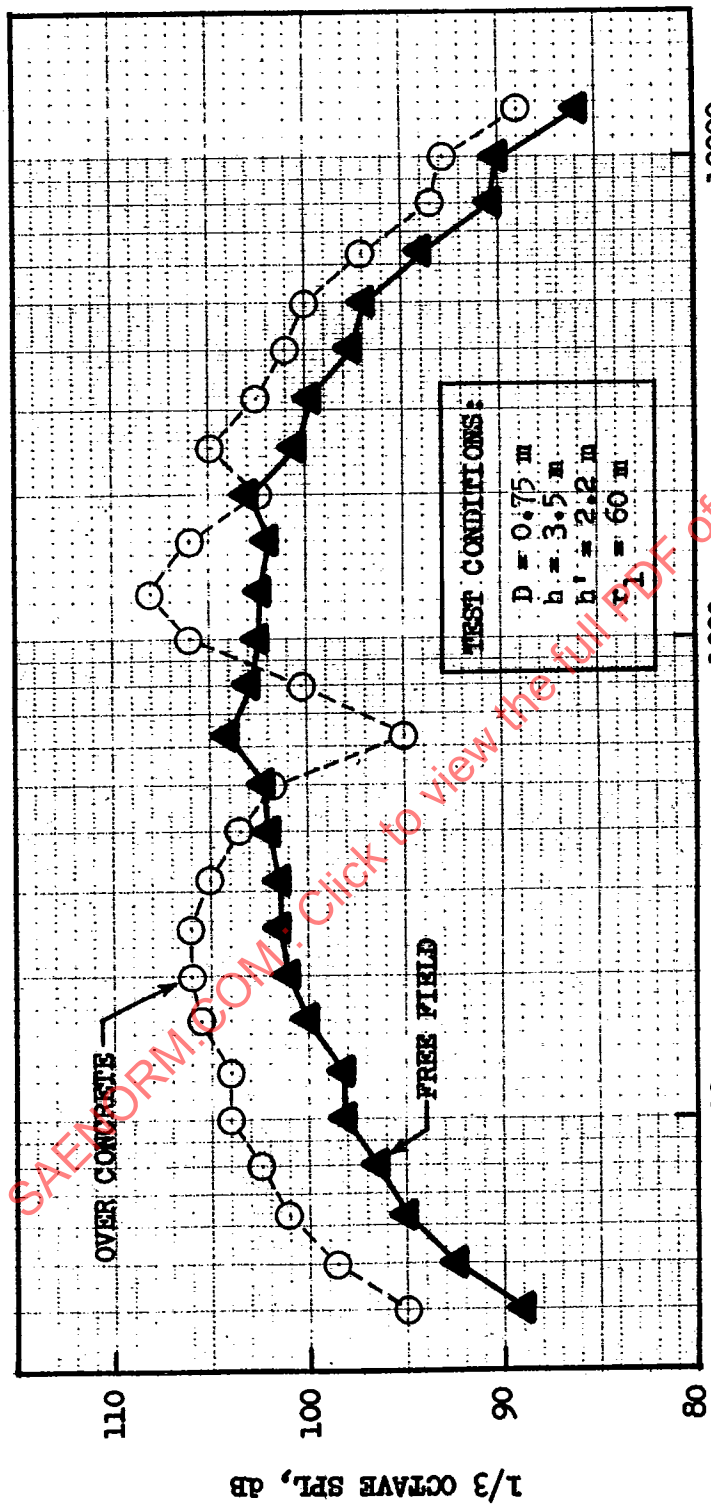


FIGURE (3-7) MEASUREMENT OVER CONCRETE CORRECTED TO FREE FIELD CONDITIONS

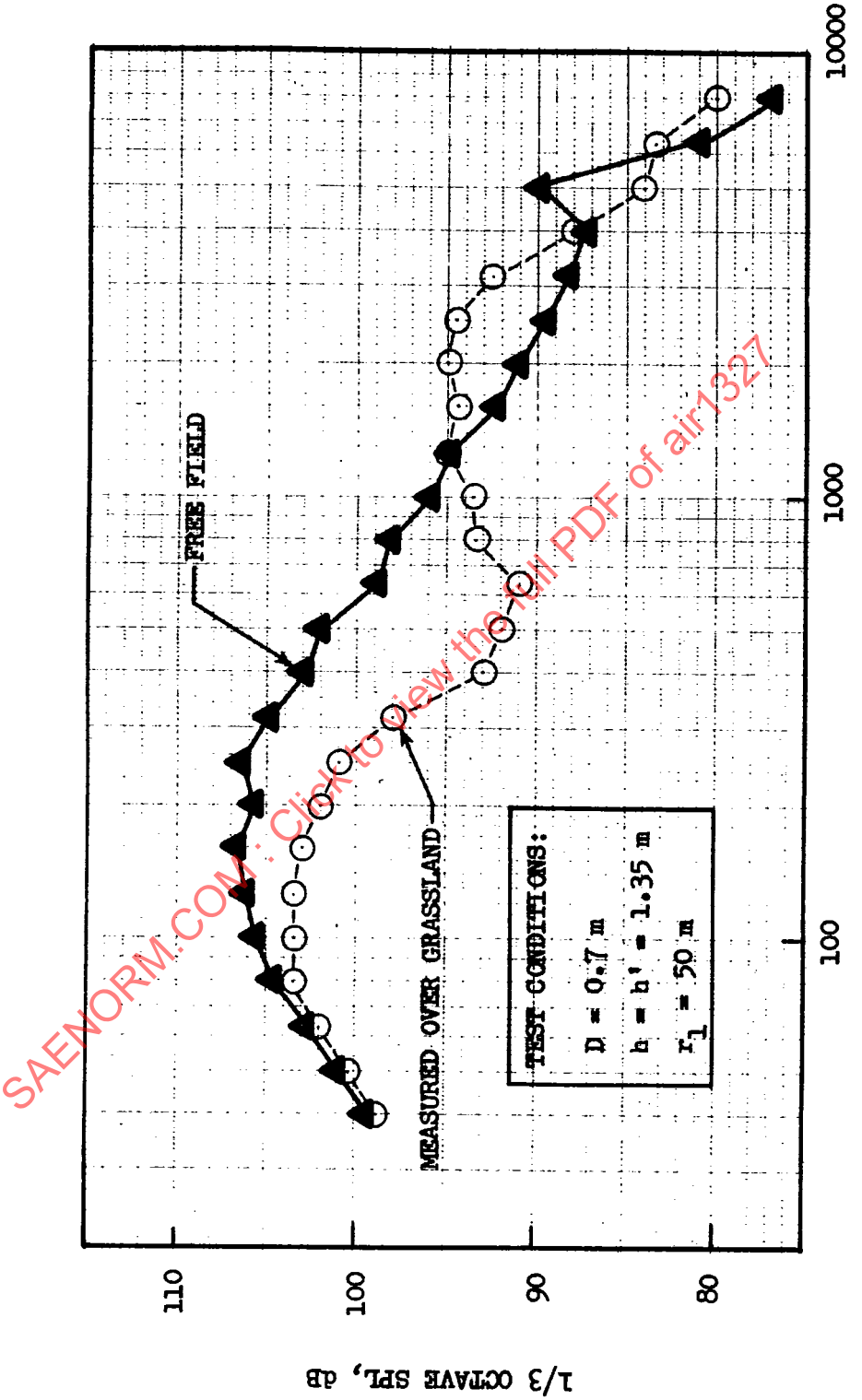


FIGURE (3-8) MEASUREMENT OVER GRASSLAND CORRECTED TO FREE FIELD CONDITIONS

### 3.3 EXPERIMENTAL METHOD FOR OBTAINING APPROXIMATE CORRECTION TO JET NOISE DATA

This section presents an experimental method for obtaining an approximate ground reflection correction to noise measurements of a broadband source of jet noise. The method consists of taking a series of "free field" measurements of a jet noise source by suspending a microphone from a balloon directly above the source, simultaneously with the taking of measurements in the reflected sound field. It is assumed that the microphone position directly above the jet exhaust would minimize sound reflected from the ground due to scattering by the jet itself and this source of error is neglected. When the balloon microphone data and the ground microphone data are adjusted to the same distance from the source (accounting for square law divergence and atmospheric absorption over any difference in the acoustic path lengths), it is possible to directly determine the reflection effects, and thus the reflection index curve.

The reflection index curve obtained in this way will apply to a unique source - ground microphone geometry (path length difference and reflected ray incidence angle) and surface condition. If an experiment were run with a different geometry, or surface, it would be necessary to repeat the balloon microphone measurement to obtain a new reflection index curve. This limitation is necessary until more reliable methods of estimating surface impedance are developed.

Ground microphone data for a jet engine source are normally taken at various angles to the inlet axis. Since the sound spectrum for an engine changes appreciably with angle from the axis, the balloon data can rigorously be compared only with the ground data taken at a microphone angle which is the same as the angle of the balloon microphone. Then the spectral content of the two measurements is approximately the same.

If the above conditions are met, the reflection index curve obtained for a jet noise source for a given geometry and surface should be applicable to sources of different noise level or spectral distribution with the same geometry and surface. This is because the ratio of free field pressure to ground-measured pressure at a given frequency should remain constant no matter what the level of the source. The reflection index curve is a measure of this ratio in logarithmic form.

A number of balloon-microphone experiments were performed with a jet noise source, keeping the ground measurement geometry and ground surface conditions constant, but varying the strength of the source. The measurement geometry is diagrammed in Figure (3-9). The surface in this case is crushed rock with a characteristic dimension of about one inch.

This procedure gave a series of curves comparing the free field pressure level to the reflected level, of which Figure (3-10) is a typical example. Data were analyzed in 1/3 octave bandwidths.

The reflection index curves for all runs were plotted and, since, theoretically, all curves should be identical, the variation at a given frequency gives an indication of the scatter in the data caused partially by variations in the surface. Figure (3-11) shows the resulting reflection index curve. This curve gives an approximate correction to jet noise data taken under equivalent geometric and surface conditions. A different geometry or surface would, of course, give a different reflection index curve.

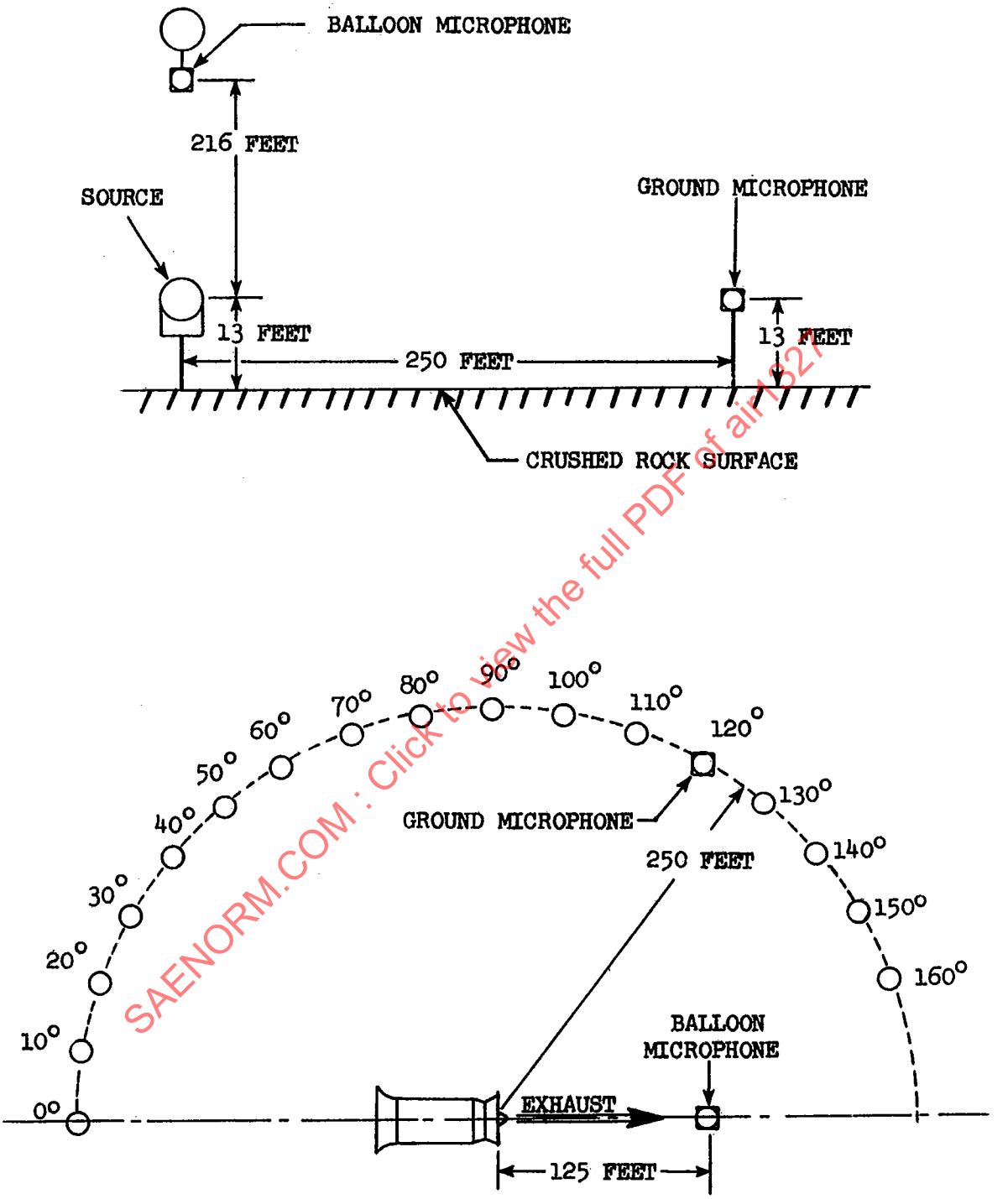


FIGURE (3-9) JET NOISE MEASUREMENT TEST GEOMETRY

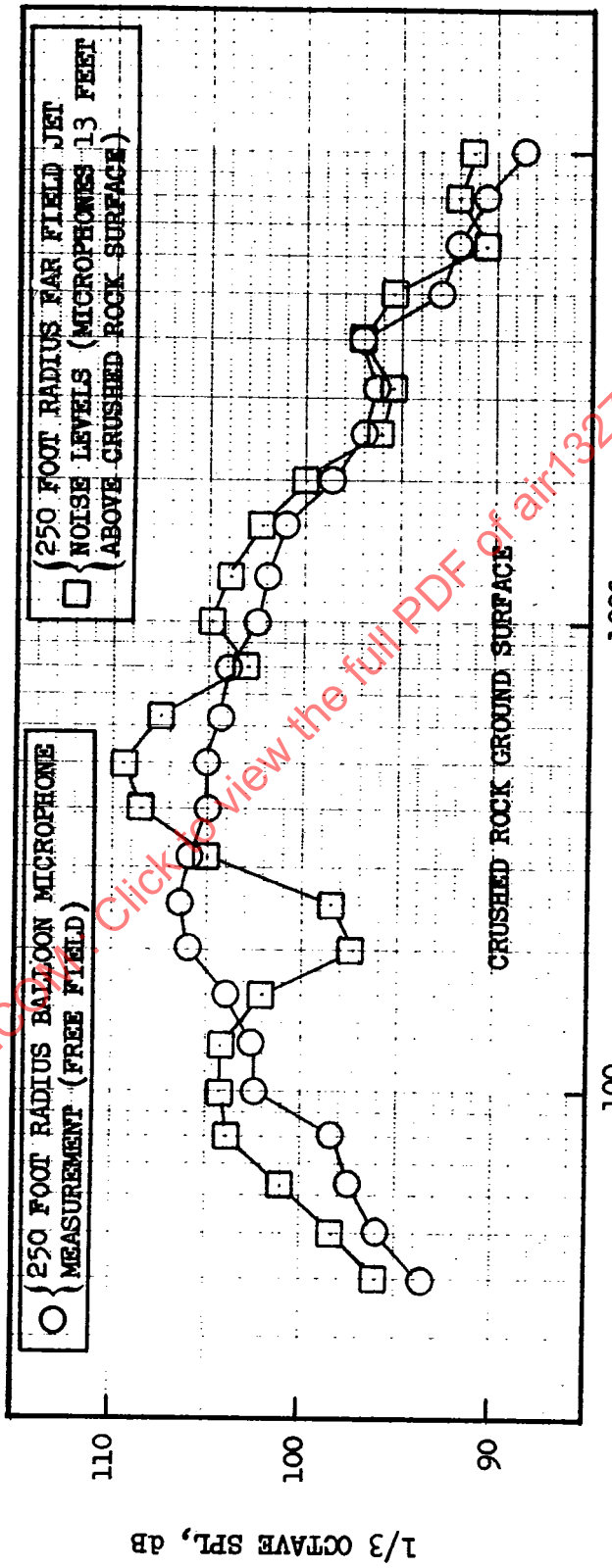


FIGURE (3-10) JET NOISE SPECTRA MEASURED AT 250 FOOT RADIUS

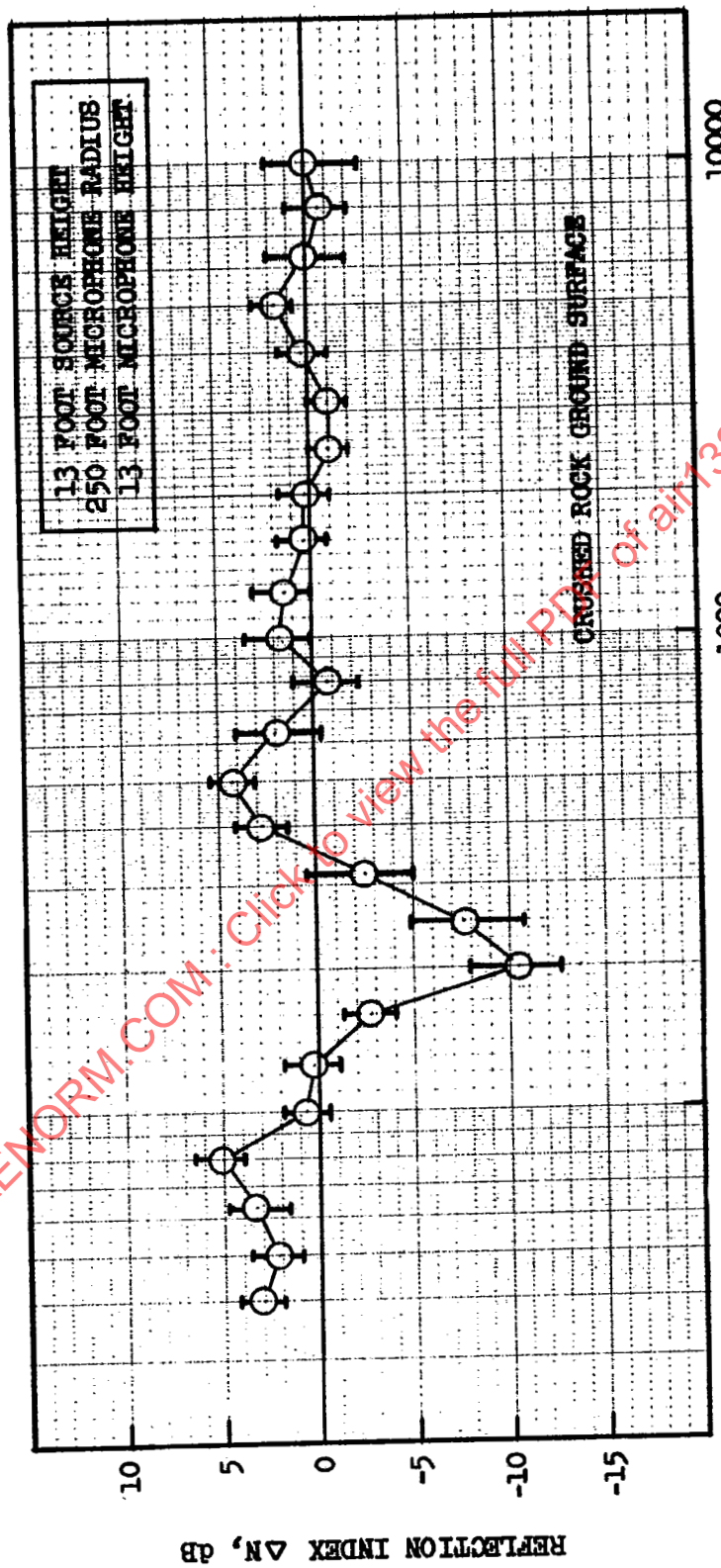


FIGURE (3-11) EXPERIMENTAL 1/3 OCTAVE JET NOISE REFLECTION INDEX CURVE SHOWING SCATTER IN MEASURED DATA

## 4. APPLICATION TO COMPLEX SPECTRA FROM TURBOFAN ENGINES

### 4.1 INTRODUCTION

The correction (due to a reflecting surface) of sound pressure level spectra from turbofan engines is complicated by the presence of discrete frequency pure tones which may protrude above the continuous spectrum of broadband noise. As with pure broadband noise, the propagation of sound between a turbofan source and a receiver located close to the ground is affected by wind and temperature gradients, ground reflection and absorption, air absorption, and ground scattering effects, among others. These phenomena occur in addition to the normal inverse square law decay of spherical waves and exist in combinations which make identification and correction very difficult. Figure (4-1) shows schematic representations of two typical spectra of a fan engine on the ground, one spectrum assumed to be measured at a distant radius by microphones near the ground and the other assumed to represent the free field spectrum.

The ground reflection effects produce a series of maxima and minima in the ground spectrum which have the following characteristics:

(1) At low frequencies the SPL's are increased, since the reflected and direct waves are always in phase because of the long wavelengths involved. This increase over the free field SPL can be as high as 6 dB, depending on the strength of the wave reflected from the ground plane.

(2) The mid-frequency range (these ranges are actually in terms of the receiver height and sound wavelength ratio) is characterized by a series of maxima and minima which are the result of the direct and reflected wave being in and out of phase. The nulls are reduced in severity as the frequency is increased due to the effect of increasing bandwidth. However, at the blade passing frequency the reflection null has reduced this one-third octave band to the broadband noise level. When pure tones are present, regardless of the frequency, the "depth" of the null is limited only by the strength of the reflected wave and the sound level of the broadband noise.

(3) Finally, at high frequencies the spectrum near the ground is increased relative to the free space spectrum by a roughly constant amount, again fixed by the absorption characteristics of the ground plane. For a perfect reflector this difference is + 3 dB.

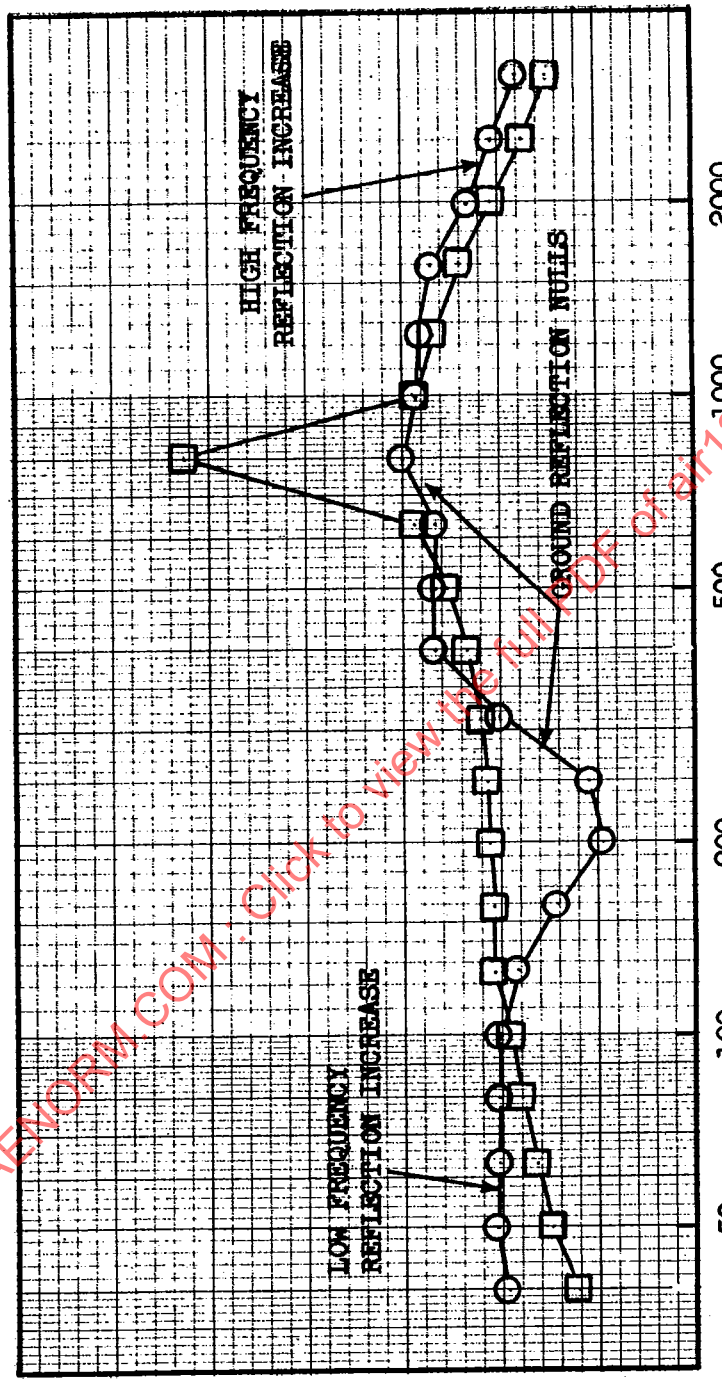


FIGURE (4-1) EFFECT ON SPL SPECTRUM PRODUCED BY GROUND PLANE (SCHEMATIC)

A variation of the reflection effect occurs for ground surfaces which are not perfect acoustic reflectors, and thus absorb a certain percentage of sound energy which strikes the surface. The results in this case are strongly dependent on the value of the surface reflection coefficient, Q, which is determined by the acoustic impedance of the surface and wave incidence angle. Generally, however, it can be stated that the ground absorption tends to shift the frequencies of corresponding peaks and nulls to lower values than those for a perfect reflector, and causes a large loss in the spectrum for a range of frequencies about the first null.

Surface winds not only produce ground turbulence, which results in scatterings and time unsteadiness of the acoustic wave, but also affect the ground reflection phenomena in a rather complicated manner. Some evidence of these complex phenomena have been found in the engine test stand acoustic data taken to date. These ground effects produce problems in two major areas. First, since poor data repeatability is caused by some of the propagation effects, it is difficult to determine small differences in noise produced by configuration changes. Second, when these effects are ignored it is impossible to extrapolate data taken at one measuring radius to a distance far from the source with any accuracy.



## 4.2 ANALYSIS APPROACH

This section presents two possible methods for making ground reflection corrections to turbofan noise spectra. The first is an outline of a rigorous method which would be more difficult in application, as it requires a determination of reflection index curves for both broadband and pure tone spectra for a given surface and geometry. This is an ideal method which would be useful only if some method is available to obtain representative reflection index curves. The second method is an approximate method, the assumptions of which may give adequate results under certain practical conditions.

Descriptions of further work on methods of reflection correlation for complex spectra containing tones, covering both theoretical and experimental results, are found in References 7, 8 and 9. These studies deal primarily with surfaces that are essentially perfect reflectors, and present some comparisons of experimental data with the developed theoretical predictions. As noted in Section 6 of this report, the factors introduced by partially absorbent surfaces are not yet fully understood or predictable, and many of the recommendations for future research in Section 6.2 deal with this phase of the ground reflection problem.

4.2.1 Outline of Methods for Correcting Complex Spectra to Free Field

Since the broadband spectrum is continuous with frequency, its correction for reflection presents no special problems, as long as the correct reflection index curve for the broadband noise is available. The pure tones, however, are a series of peaks at certain discrete frequencies, so that their correction presupposes an advanced knowledge of the pure tone generation frequencies.

To apply this method, it is necessary to have the data in the form of a narrow band spectrum, say a 50 Hz constant bandwidth. For most cases the pure tone peaks will protrude noticeably above the broadband level of the narrow band data (the peaks may not be as obvious for 1/3 octave data, depending on the properties of the source). Reflection effects, however, may lower the level of the pure tone peak to such an extent that it is being masked by the broadband level, and this is the reason why it is important to determine the expected pure tone frequencies and their harmonics using engine rpm and blade number.

If, at a certain frequency, a pure tone peak did not protrude noticeably above the broadband level, the possibility exists that reflection effects have reduced the pure tone level below the broadband, in which case it is impossible to obtain the actual pure tone level from this set of data. One remedy to this situation would be to rerun the case with a different microphone location, giving a new reflection geometry (path length difference) such that there would be less cancellation at this frequency, and the pure tone peak would become evident. One possibility would be to locate several microphones at each measuring angle, each at a different height from the ground. Recorded simultaneously, they would show reflection nulls at different frequencies in the spectrum. Superposition of the spectra measured at the different heights will often permit the reflection effects to be recognized.



If the above conditions are met, a typical turbofan spectrum such as that shown in Figure (4-2) could be corrected by the procedure outlined below:

First, it is necessary to have a measurement of broadband spectra with all pure tones electronically filtered out (note that this again would require knowledge of pure tone frequencies). This curve would contain only the broadband noise levels, and could be corrected by the broadband reflection index curve, as shown in Figure (4-3).

Second, the pure tone levels are corrected independently, using the pure tone reflection index curve. The corrected pure tone levels could then be superimposed upon the corrected broadband levels to give the overall corrected turbofan spectrum, as illustrated in Figure (4-4).

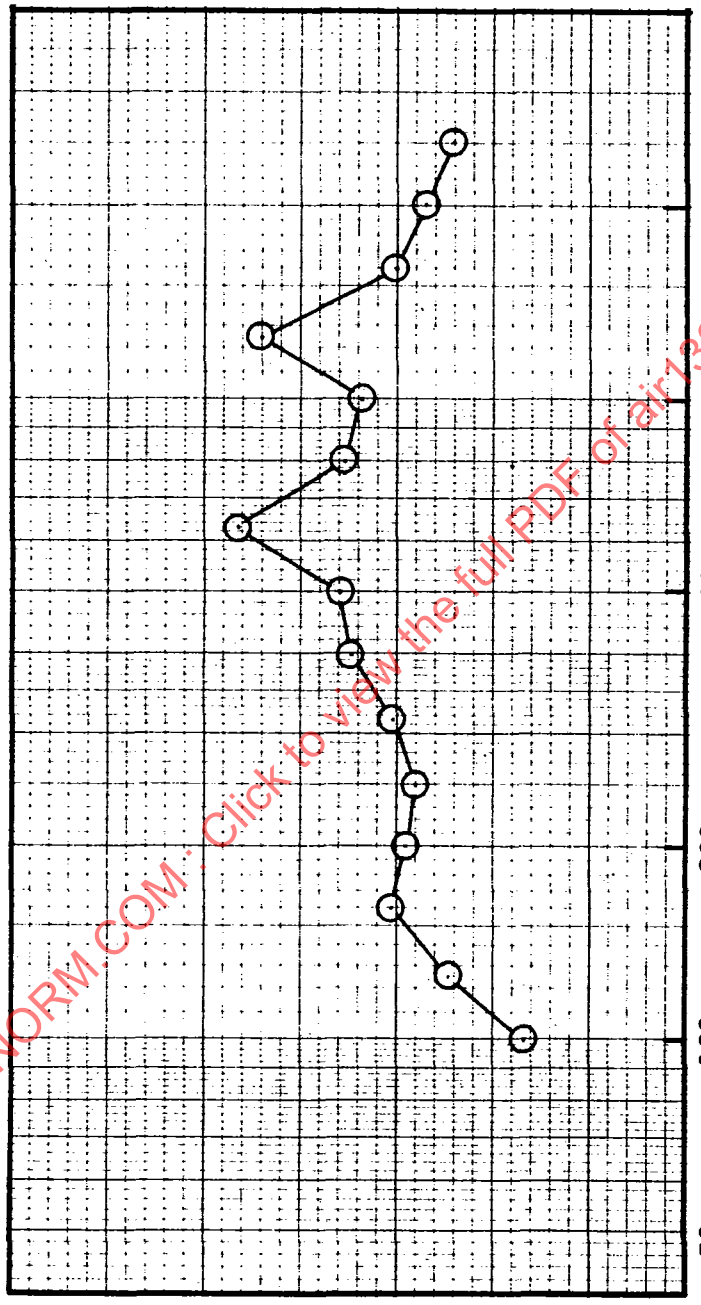


FIGURE (4-2) MEASURED TURBOFAN SPECTRUM (SCHEMATIC)

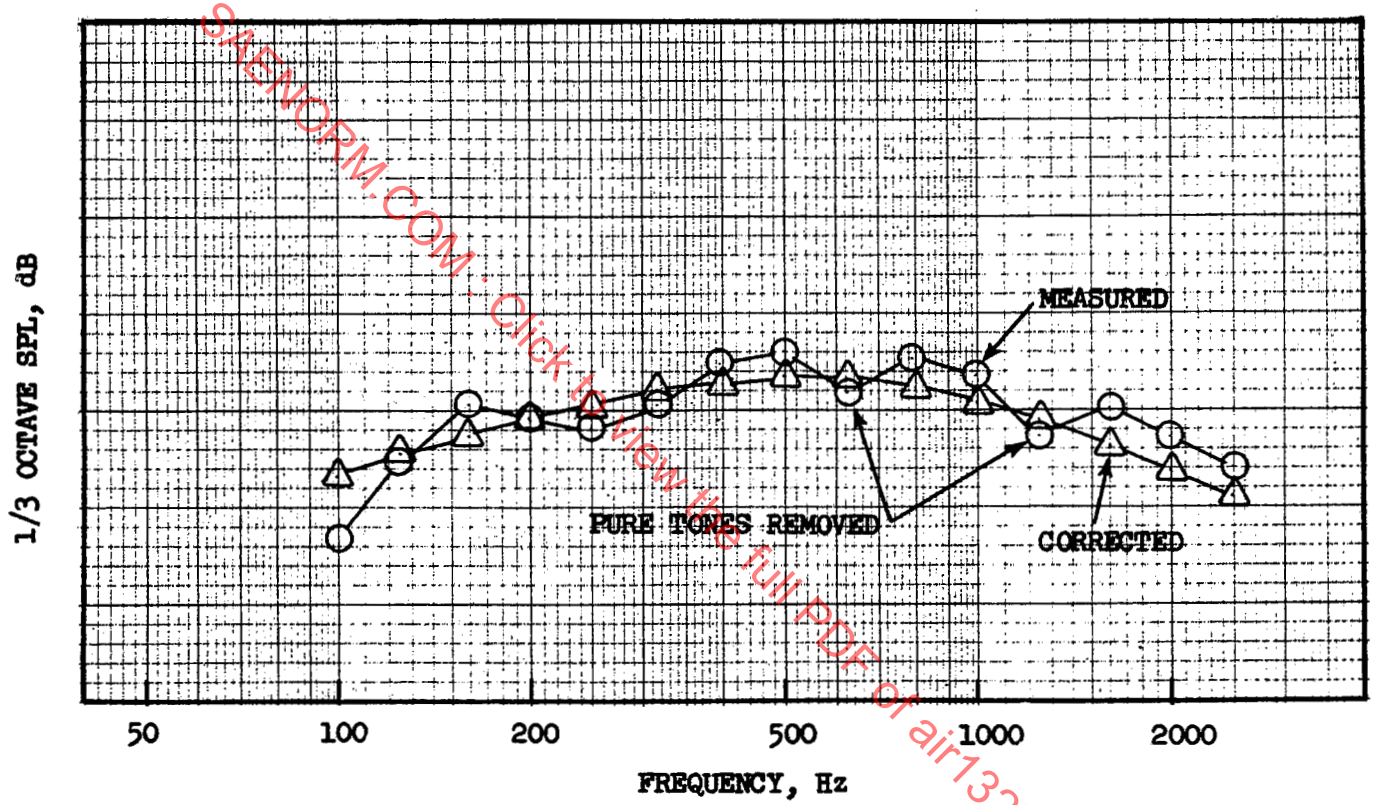




FIGURE (4-3) BROADBAND NOISE SPECTRUM CORRECTION (SCHEMATIC)

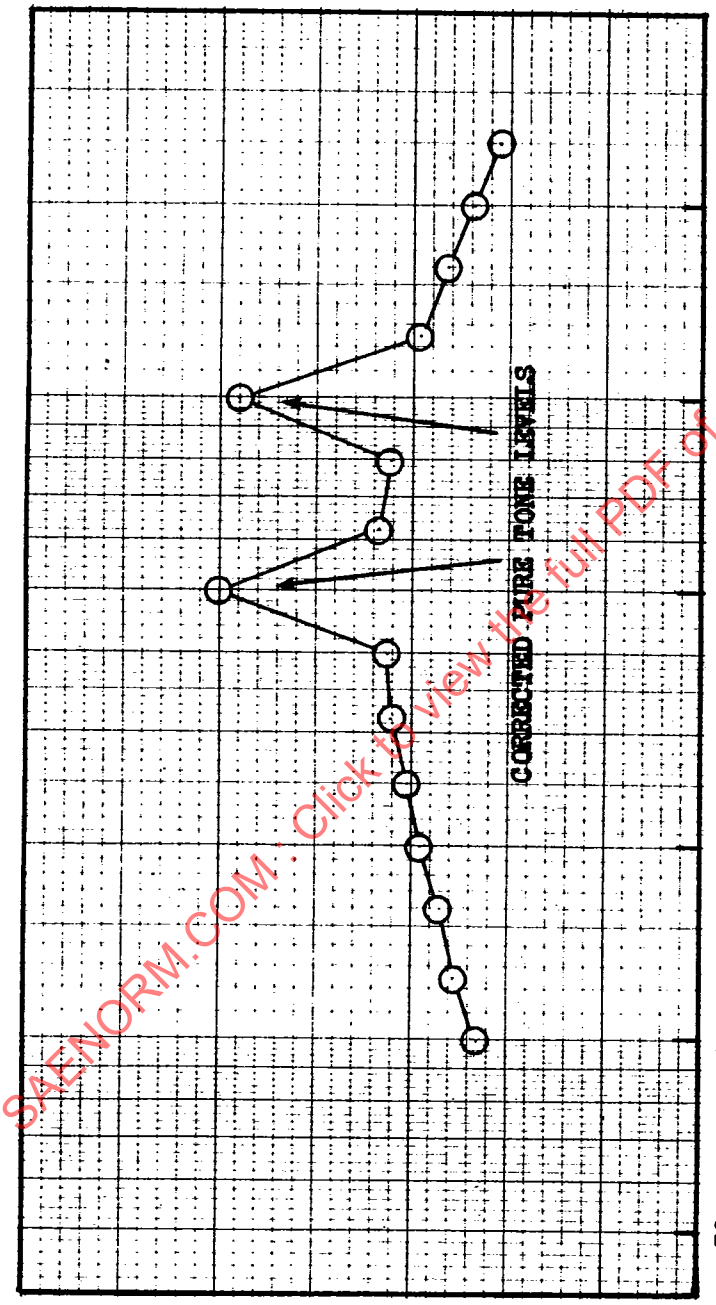


FIGURE (4-4) CORRECTED TURBOFAN SPECTRUM (SCHEMATIC)

4.2.2 Approximate Method for Correcting Turbofan Spectra

If an accurate experimentally determined reflection index curve is not available for a particular surface or source-microphone geometry, it is possible to make an approximate correction to reflection data with a minimum amount of assumptions using the method outlined below. The utilization of the method requires the ability to determine the following two pieces of information:

(1) An estimation from the measured pressure reflection pattern of the first few frequencies of the reflection peaks and nulls.

(2) An estimation of the magnitude of the reflection coefficient, /Q/, of the surface.

The reason for requiring the above information is to facilitate calculating the reflection index curve from an approximate curve of the complex reflection coefficient, Q. Possible methods of obtaining these curves will be considered later.

From the peak and null reflection frequencies the argument of the reflection coefficient, $\delta$, is obtained. A different value of $\delta$ will be obtained at each frequency, and this will give an approximation of the variation of $\delta$ with frequency. Instead of calculating $\delta$ directly, it has been found more convenient to introduce an intermediate variable, $\phi$, which will be called the phase factor. The phase factor $\phi$ is related to $\delta$ through the time lag of the reflected ray, $\tau$. The effective time lag is related to an effective path length difference, $\Delta r'$, by the relation

$$\tau = \frac{\Delta r'}{c} \tag{4.1}$$

where $\Delta r'$ includes not only the actual geometric path length difference but also effective changes in this length arising from phase shift effects upon reflection from a finite impedance surface or curvature of the path due to atmospheric inhomogenieties. $\phi$ is then defined as the ratio of the geometric path length to the effective path length,

$$\phi = \frac{\Delta r}{\Delta r'} \tag{4.2}$$

If $\phi = 1$, the surface is a perfect reflector and the atmosphere is homogeneous.

The condition for the occurrence of a reflection null at a wavelength $\lambda$ is

$$\Delta r' = \lambda\frac{n}{2} \quad , \quad (n - \text{odd}) \tag{4.3}$$

or, in terms of $\delta$

$$\delta - 2\pi\frac{\Delta r}{\lambda} = n\pi \quad , (n - \text{odd}) \tag{4.4}$$

Thus, we can write

$$\frac{2\pi\ \Delta r'}{\lambda} = \frac{2\pi\Delta r}{\lambda} - \delta \tag{4.5}$$

or

$$\frac{2\pi\ \Delta r}{\phi\ \lambda} = \frac{2\pi\ \Delta r}{\lambda} - \delta \tag{4.6}$$

So that

$$\delta = \frac{2\pi\Delta r}{\lambda}\ (1 - \frac{1}{\phi}) \tag{4.7}$$

where, again, $\Delta r$ is the actual geometric path length difference and $\lambda$ is the wavelength at which the null experimentally occurs (it can be shown that Eq. (4.7) also applies to reflection peaks). Combining Eq. (4.2) and Eq. (4.3), we get the simple expression for $\phi$,

$$\phi = \frac{2\Delta r}{n\lambda} \quad , \quad (n - \text{odd}) \tag{4.8}$$

for reflection nulls, or we would find

$$\phi = \frac{\Delta r}{n\lambda} \quad , \quad (\text{any } n) \tag{4.9}$$

for reflection peaks.

When the frequencies of peaks and nulls are determined from the experimental data, Equation (4.8) or (4.9) can be used to find $\phi$, which can then be plotted as a function of frequency. This plot can be used, then, to find the approximation to $\delta$ at any frequency. (Note: It has been found more advisable to plot $\phi$ rather than $\delta$ because $\phi$ was more generally a monotonically varying function of frequency, and could be represented analytically by straight line segments for purposes of calculation).

A simpler assumption for $\phi$ might have been to let $\phi$ equal some constant average value over the frequency range. This is a reasonable assumption for higher frequency ranges (>2000 Hz), but tends to introduce large errors in lower ranges where reflection effects are strongest in typical turbofan cases, and the location of the strong peaks and nulls are very sensitive to changes in $\phi$ in this region.

Calibrating the site by determining the magnitude of the reflection coefficient /Q/ is, in general, a more difficult problem. Since it is assumed that the actual impedance of the surface is not obtainable, /Q/ must be found from correlations with earlier data taken with the same surface and (preferably) equivalent geometry.

One possibility would be to use a loudspeaker as a sound source and simultaneously record the reflection pattern at two geometries, one in the farfield with the same geometry (radius, angle, and height) as that used in engine tests, and a second microphone at the same angle but at a radius much closer to the source and located at a height such that it falls on the line directly between the center of the source and the farfield microphone. The near microphone would have a much larger path length difference than the farfield microphone, which has two effects. First, the predominant reflection effects at the near microphone would be forced into a lower frequency range, possibly below that of interest. Second, the reflected signal will be well below the direct signal if the reflected distance is much greater than the direct distance. Thus, across the major part of the range of frequencies, the general additive term from the reflected signal is very low with respect to the direct level, and for the purposes of the following approximate procedure, can be neglected. (For example a near microphone at 10 feet distance with both the source and microphone at 12 foot heights would have only about one dB added to the direct level above the first few null/reinforcements.)



When the near microphone levels are extrapolated out to the radius of the reflection measurement, an approximate reflection index curve can be obtained directly. Values of /Q/ can then be found from the analytical expression for the reflection index curve, Eq. (2.7). It was found that in general the assumption of a constant value of /Q/ throughout the frequency range did not lead to excessive errors. It should also be remembered that the reflection index curve is likely to be quite sensitive to the angle the reflected wave makes with the ground, particularly near grazing incidence, so that values of /Q/ found at certain angles of incidence may not apply to appreciably different angles.

After the approximate values of /Q/ and δ are determined, a reflection index curve can be calculated from the appropriate form of Eq. (2.7). This correction can then be applied to the sound pressure level reflection pattern to give an approximation to the pressure spectra which would be measured at a given radius with no reflection effects (free field).

### 4.2.3 Application of Approximate Method

The following example illustrates the above procedure for a turbofan located at a height of 12 feet above a measuring plane of crushed rock and serves to give an indication of the validity of the procedure. The reflection patterns were measured simultaneously at two different radii, 150 feet and 250 feet, with both microphone heights at 12 feet. The path length difference, then, was different at each microphone location, so that a different reflection correction applied in each case. The objective was to remove the reflection effects from each spectrum, and then adjust the 250 foot data back to 150 feet for comparison to the 150 foot corrected data. Any large differences in the comparison can be attributed to errors in the reflection correction introduced by the assumptions used to obtain the reflection index curve.

Figure (4-8) shows the pressure spectra of the 150 foot and 250 foot measurements, where neither have been corrected for reflection effects but the 250 foot data has been adjusted back to 150 feet by correcting for spherical divergence and air attenuation (note that it is immaterial whether these corrections or the reflection corrections are made first, since all corrections are additive terms. Close examination of Figure (4-8) allows one to make reasonably good guesses as to the approximate frequency of the reflection peaks and nulls. These were chosen as:

150 Feet

1st Null, ~200 Hz
1st Peak, ~450 Hz
2nd Null, ~800 Hz
2nd Peak, ~1000 Hz

| | |
|---|---|
| 250 Feet | 1st Null, ~250 Hz |
| | 1st Peak, ~630 Hz |
| | 2nd Null, ~1000 Hz |
| | 2nd Peak, ~1600 Hz |

These values lead to the approximate $\phi$ - curves shown in Figure (4-5).

Extensive testing over the crushed rock surface, including a number of correlations with jet noise balloon data and loudspeaker experiments, have pointed to an approximate average value of the magnitude of the reflection coefficient of /Q/ = .5. When this is used with the $\phi$ - curves of Figure (4-5), the reflection index curves of Figures (4-6) and (4-7) are obtained. The calculation is based on the reflection index expression for 1/3 octave broadband noise, Eq. (2.15).

The use of this equation inserts an additional assumption, that the complex spectrum from turbofan noise measurements can, to an initial approximation, be corrected as if it were broadband. This correction will be the least accurate in the third octave which contains the pure tone fundamental (4000 Hz in this case). However, since most of the strong reflection effects have leveled off before the pure tone fundamental is reached, the errors introduced should be relatively small.

The corrected spectra are shown in Figure (4-9). The collapse of these curves is generally good, with the difference being greater than 1.5 dB at only 5 of the 1/3 octave central frequencies, compared with 11 points of the uncorrected data. The standard deviation of the uncorrected data, found by taking the square root of the sum of the squares of the differences in dB at each 1/3 octave center frequency, was 2.3 dB, while that for the corrected data was 1.6 dB.

The method for improving the data collapse, of course, is to obtain a more accurate representation of the complex reflection coefficient as a function of frequency for the case being considered, leading to a better reflection index curve.

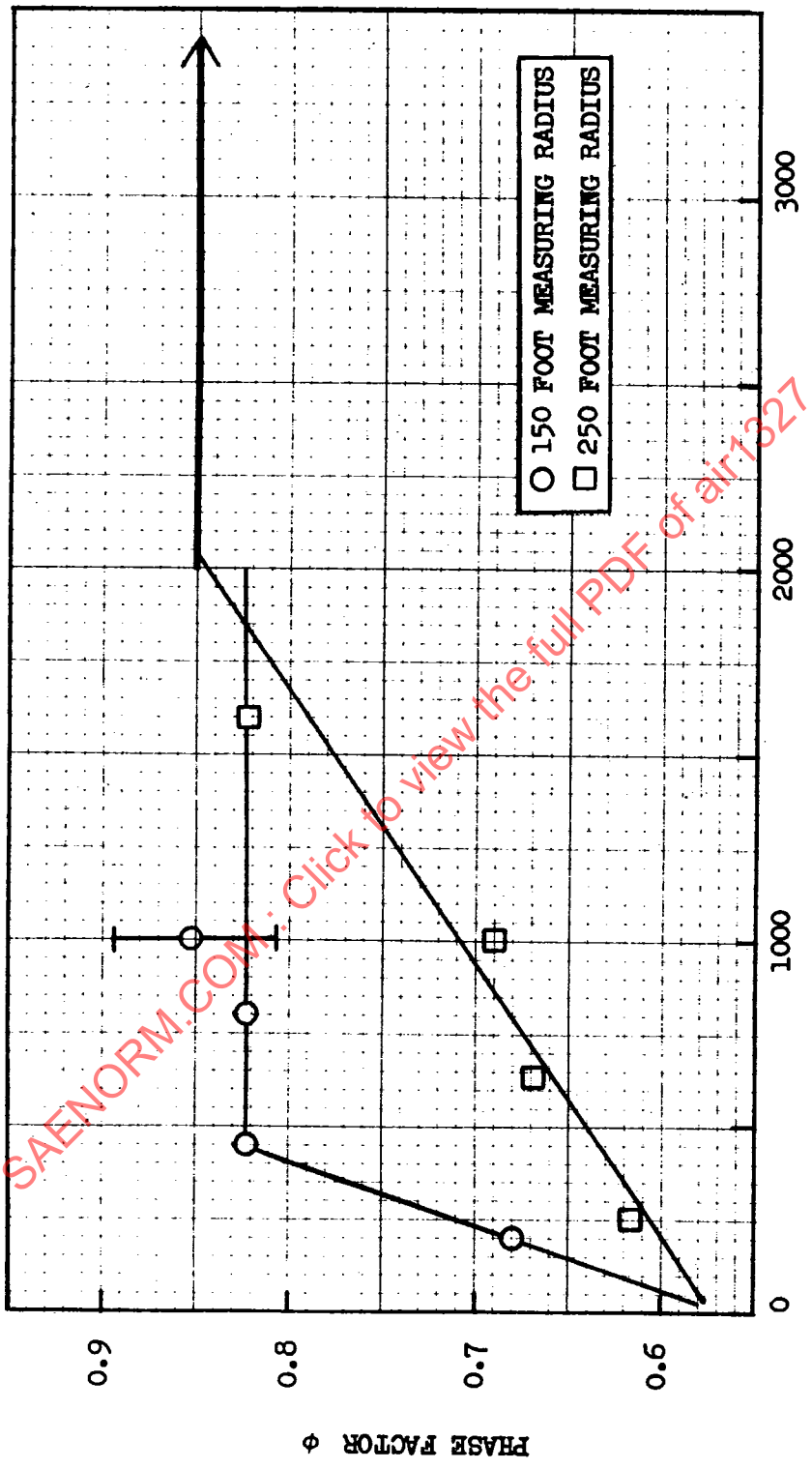


FIGURE (4-5) PHASE FACTOR APPROXIMATION vs. FREQUENCY FOR A TURBOFAN SOURCE OVER CRUSHED ROCK SURFACE

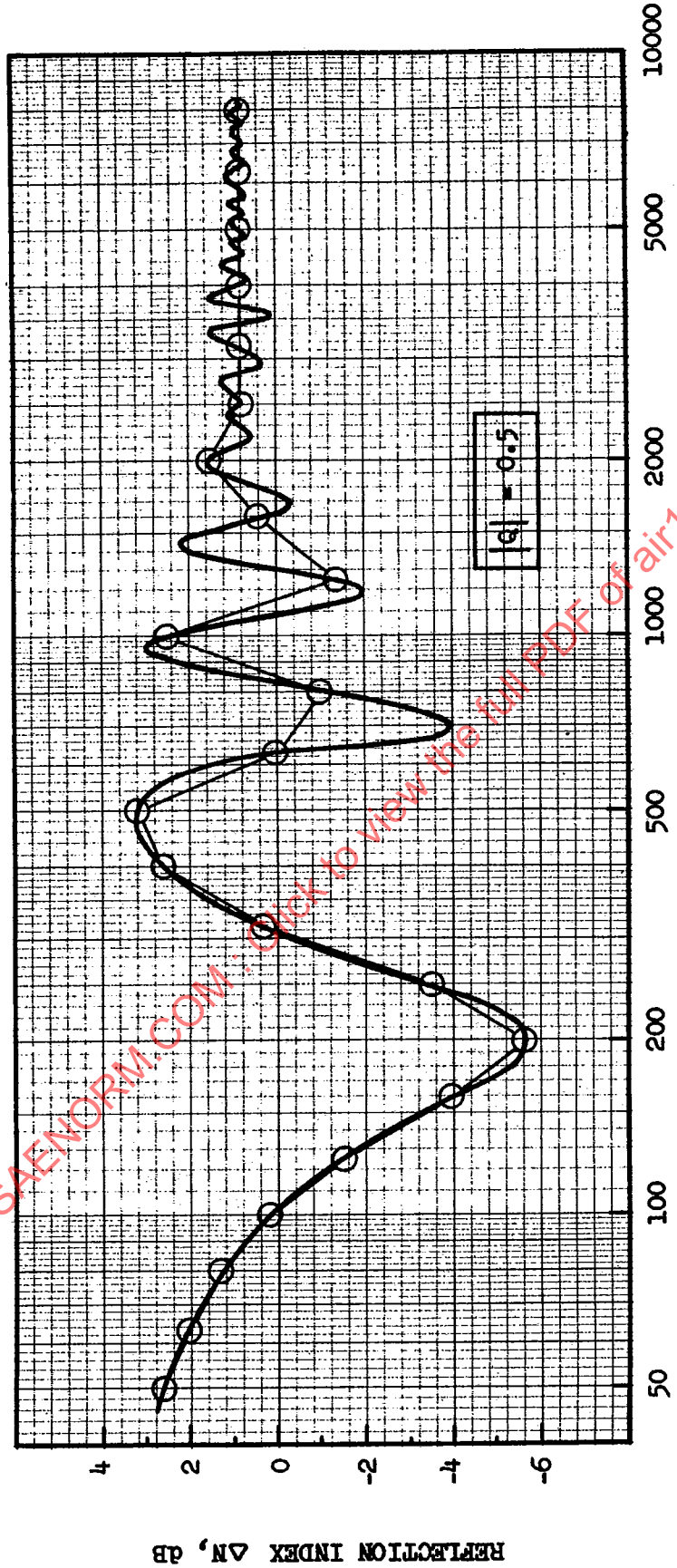


FIGURE (4-6) REFLECTION INDEX CURVE FOR 150 FOOT MICROPHONE RADIUS

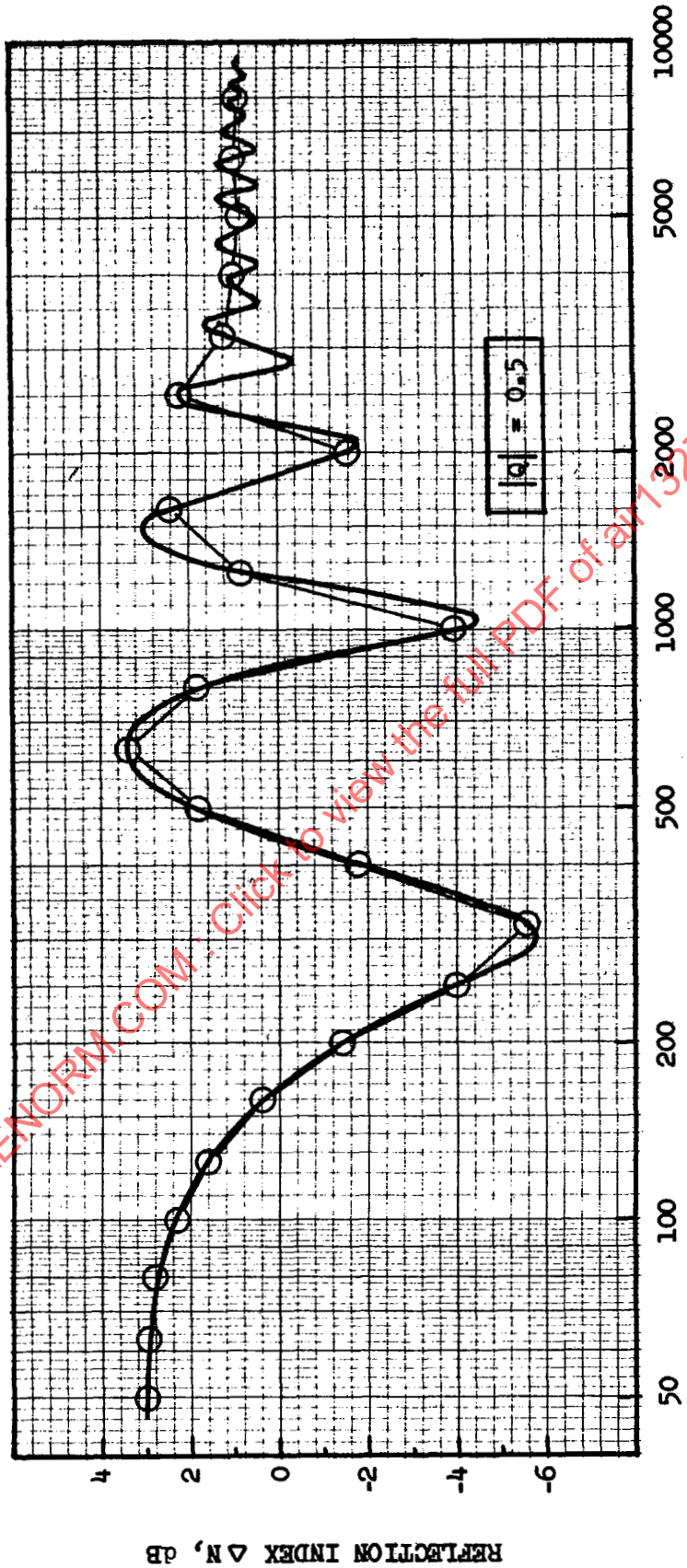


FIGURE (4-7) REFLECTION INDEX CURVE FOR 250 FOOT MICROPHONE RADIUS

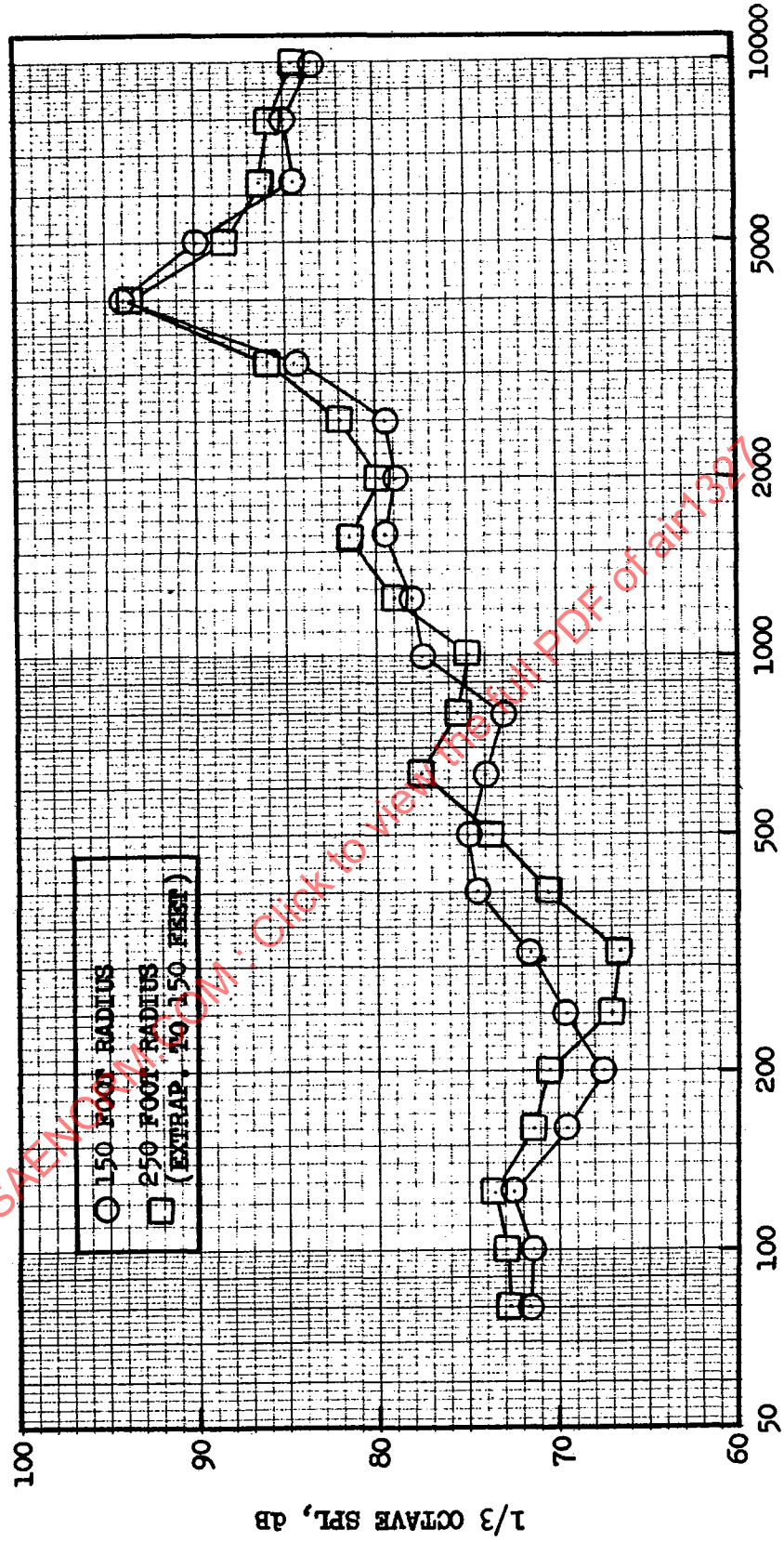


FIGURE (4-8) PRESSURE SPECTRA UNCORRECTED FOR REFLECTION
250 FOOT DATA EXTRAPOLATED TO 150 FOOT RADIUS

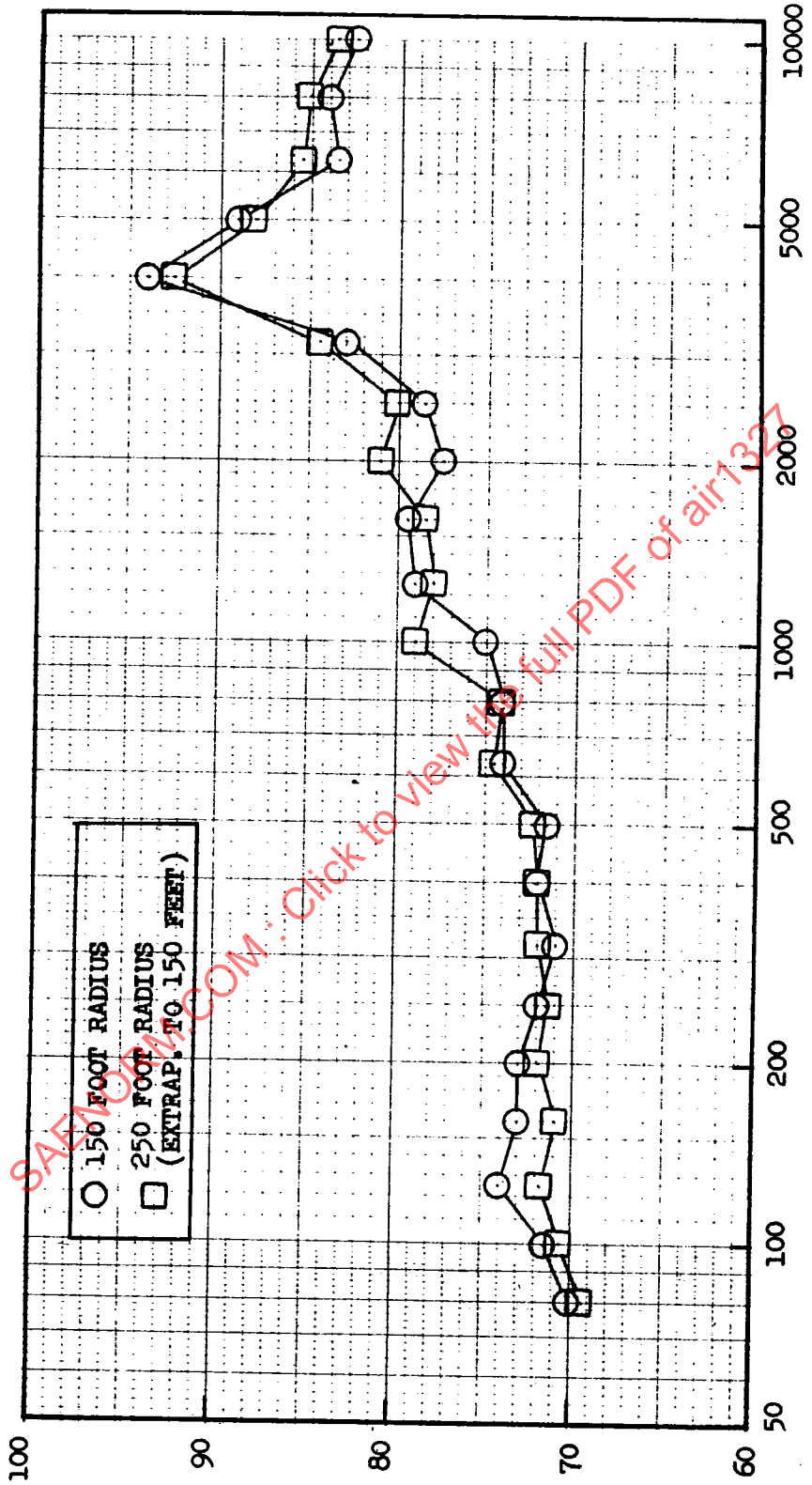


FIGURE (4-9) PRESSURE SPECTRA CORRECTED FOR REFLECTION
250 FOOT DATA EXTRAPOLATED TO 150 FOOT RADIUS

## 5. METHODS TO MINIMIZE GROUND REFLECTION EFFECTS

### 5.1 EXPERIENCE WITH HIGH RECEIVER HEIGHTS

When the difference in path length between the direct and the reflected ray is large with respect to the wavelength of the particular signals of interest, several beneficial effects result that may be used to minimize the problems of ground reflection effects on data. First, an increase in path length difference shifts the major null patterns (first through third) to lower frequencies, and in the testing of scale models, this shift may be selected so that these null patterns are below the frequency range of interest. Figure (5-1) illustrates this type of shift for an 8:1 scale model jet noise test. Since at this large scale factor, 50 Hz full scale is represented by 400 Hz in model size, the shift of the null patterns shown between curve (a) and curve (b) of Figure (5-1) provides that essentially the full spectrum of interest lies in the energy-reinforced upper frequency zone where sufficient nulls and reinforcements lie in a given 1/3 octave to provide a statistically averaged increase in the measured noise signal (this increase is +3 dB for a perfect reflector on hard surface, and ranges around 1.5 to 2 dB for gravel or typical ground surfaces. This effect is strictly true only for broadband noise.

A second effect noted with the use of large path length differences is involved with the time-variation of acoustic ray paths with wind, gusts, eddies, etc. in the ambient airmass. Over a relatively long (30 seconds) averaging time for data acquisition the path length difference will vary in some proportion to its magnitude. When the variation approaches the order of size of the wavelength of a pure tone element, a time-averaging effect will produce a random shift of the tone through both cancellations and reinforcements, and thus the averaged signal for the pure tone will approach the random-reinforcement level noted above for broadband noise. Figures (5-2) and (5-3) show the trace versus frequency of a slowly-swept pure tone, recorded by a microphone having a path length difference of 5.46 ft., at a distance of 50 feet from a speaker source. It is noted that the repetitive pattern of null and reinforcement is distinct up to approximately 1500 Hz, but above that frequency, the time-variance of the path length difference produces a random pattern of noise level variation with the sweeping frequency. These data are for a rough gravel surface; for a hard surface such as concrete, the breakdown frequency is higher

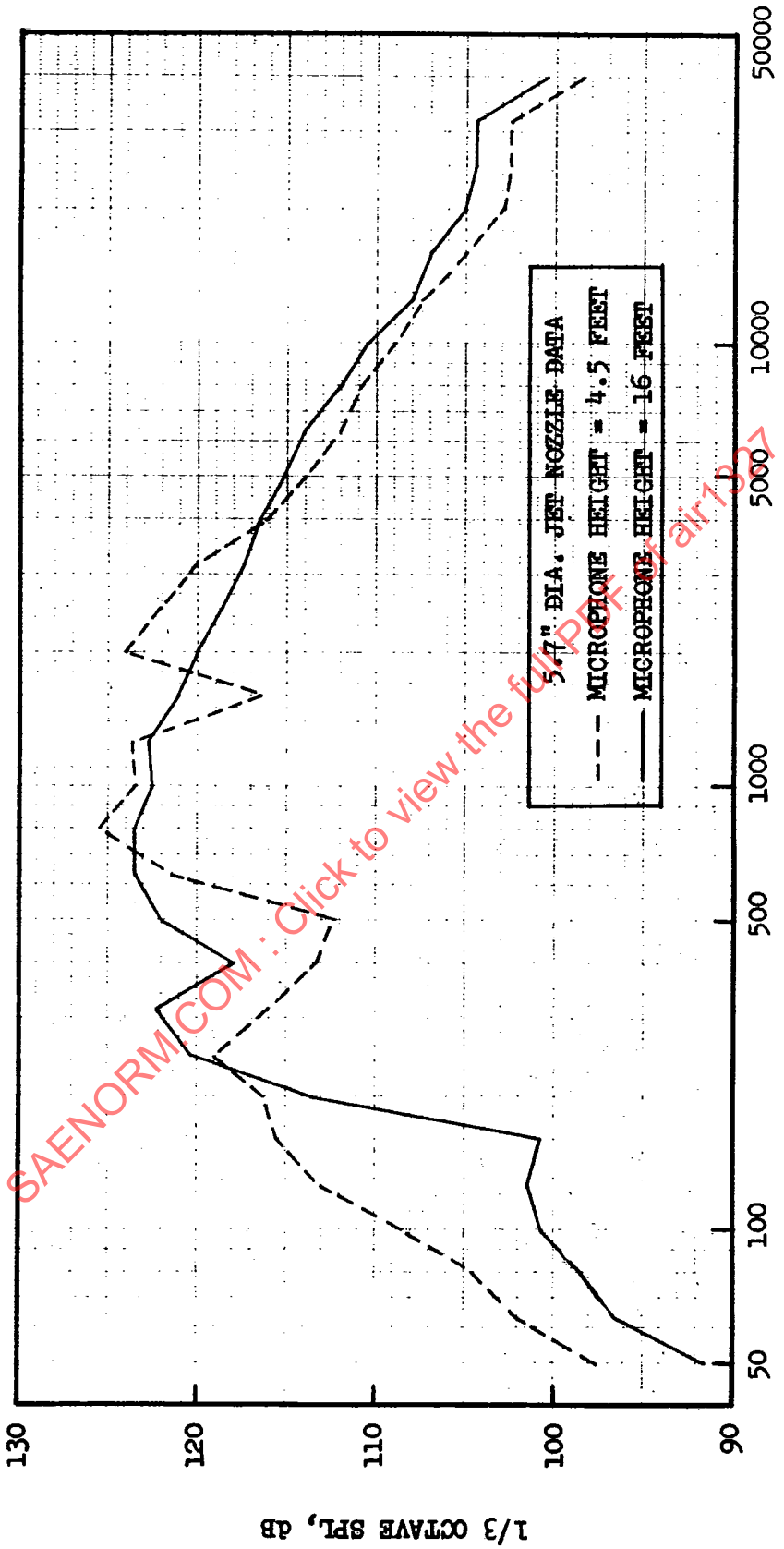


FIGURE (5-1) SHIFT IN REFLECTION PATTERN WITH RECEIVER HEIGHT VARIATION

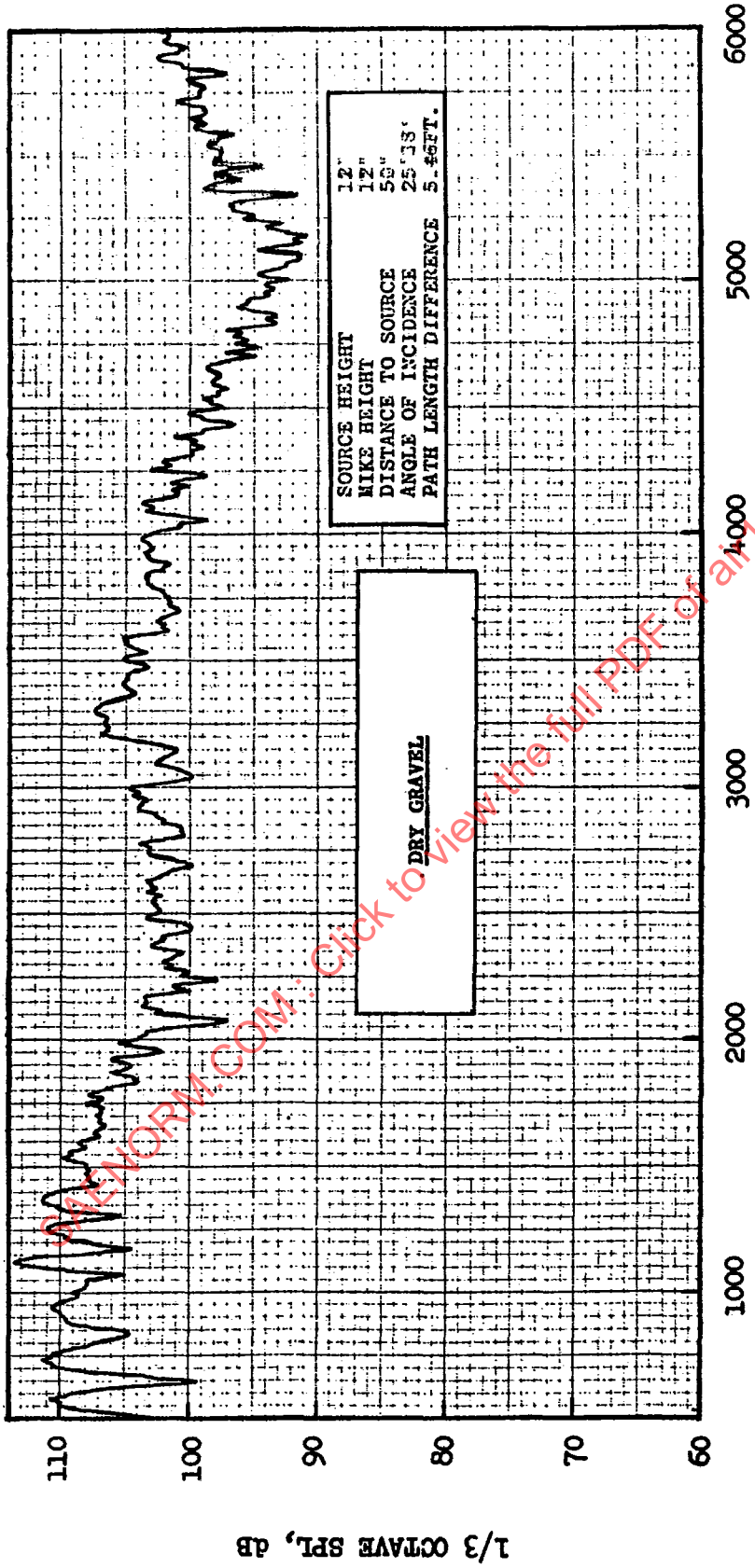


FIGURE (5-2) GROUND REFLECTION TESTS - DRY GRAVEL

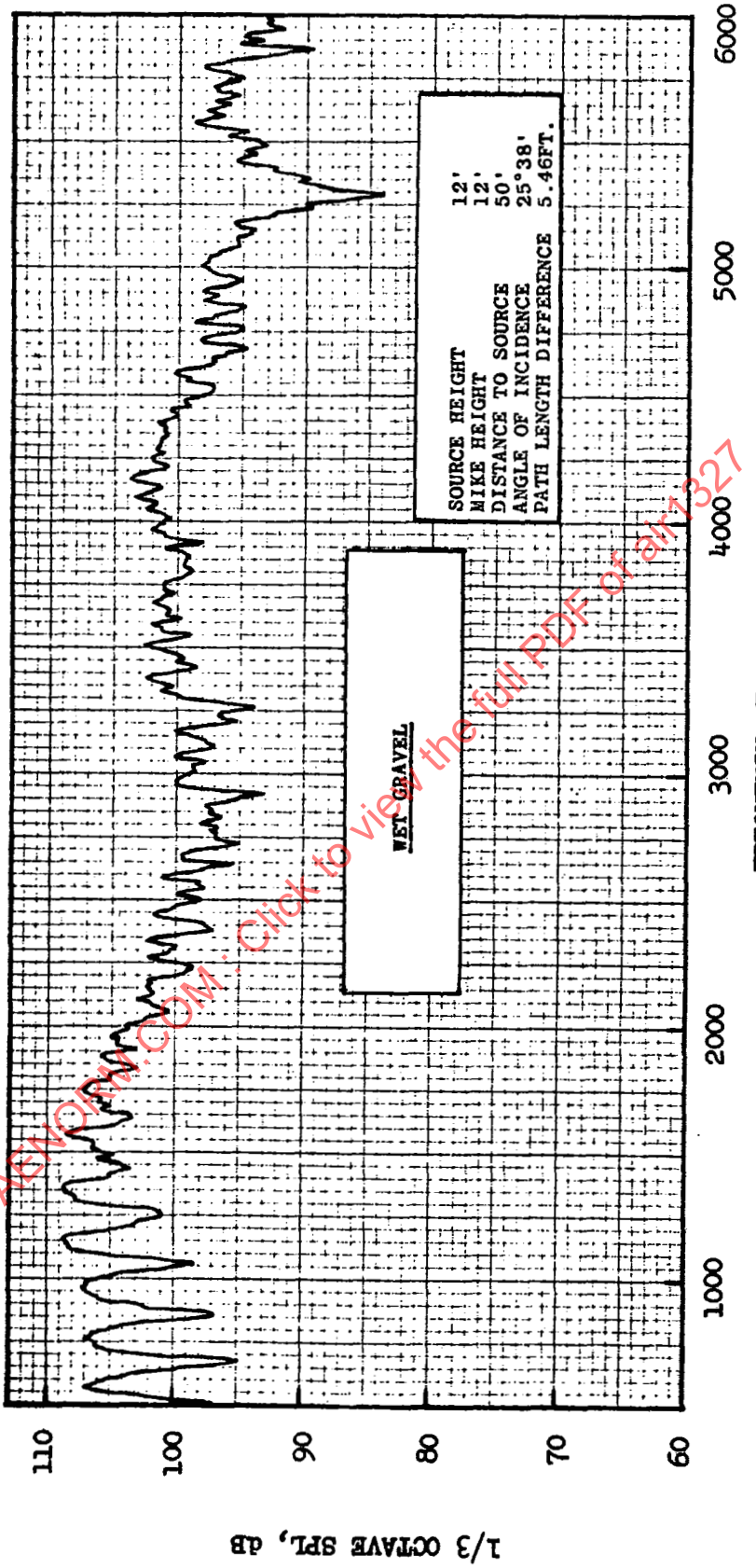


FIGURE (5-3) GROUND REFLECTION TESTS - WET GRAVEL

as shown in Figure (5-4). Further studies are discussed in Reference 6. This effect of breakdown of the reflection pattern can be utilized to obtain more statistically repeatable data for sources which have both broadband and pure tone elements.

A third advantage of the use of high receiver heights (increasing path length differences) is the designed placement of the major null patterns at selected frequencies for direct comparison with other data. The most significant use of this advantage lies in the realm of predicting flyover noise levels from ground static engine noise data. This is covered in some detail in the following section. Another potential use for deliberate path length design involves comparison of data from one site to another. Often, differences in the frequency location of null patterns make direct comparison extremely difficult; calculation of the expected null patterns of a site, based on theoretical geometric considerations and experience-derived phase factor estimates permit one to design the proper location for placement of microphones to yield a similar reinforcement null pattern to a prior set of data to which comparison is desired. Usually, source height is less easily adjusted, and the measurement arc radius is based on other considerations, leaving microphone height as the most effective means of adjusting the null pattern frequencies.

## 5.2 RECOMMENDATIONS FOR INFLIGHT NOISE PREDICTION

Flight data provides an extremely complex pattern of reflection effects from the ground plane, since the geometry of the direct and reflected paths are continually changing with time. For a four-foot microphone height, and for a flight path directly over the microphone, the path length difference will vary from a low quantity to a maximum value of 8 feet at overhead, then reduce again to a low value as the aircraft recedes. This is shown in Figure (5-5), a sketch of the geometric considerations with a table of path length difference versus angle of the arriving acoustic ray to the ground. Figures (5-6) and (5-7) show 1/3 octave SPL spectra for a series of times before (Figure (5-6)) and after (Figure (5-7)) the time of maximum overall sound pressure level. The shifting frequency of the first and second nulls is quite noticeable in these data. Both from direct listening or from listening to flyover recordings, the movement of the reinforcement between first and second null can be heard as a change in the frequency of a significant

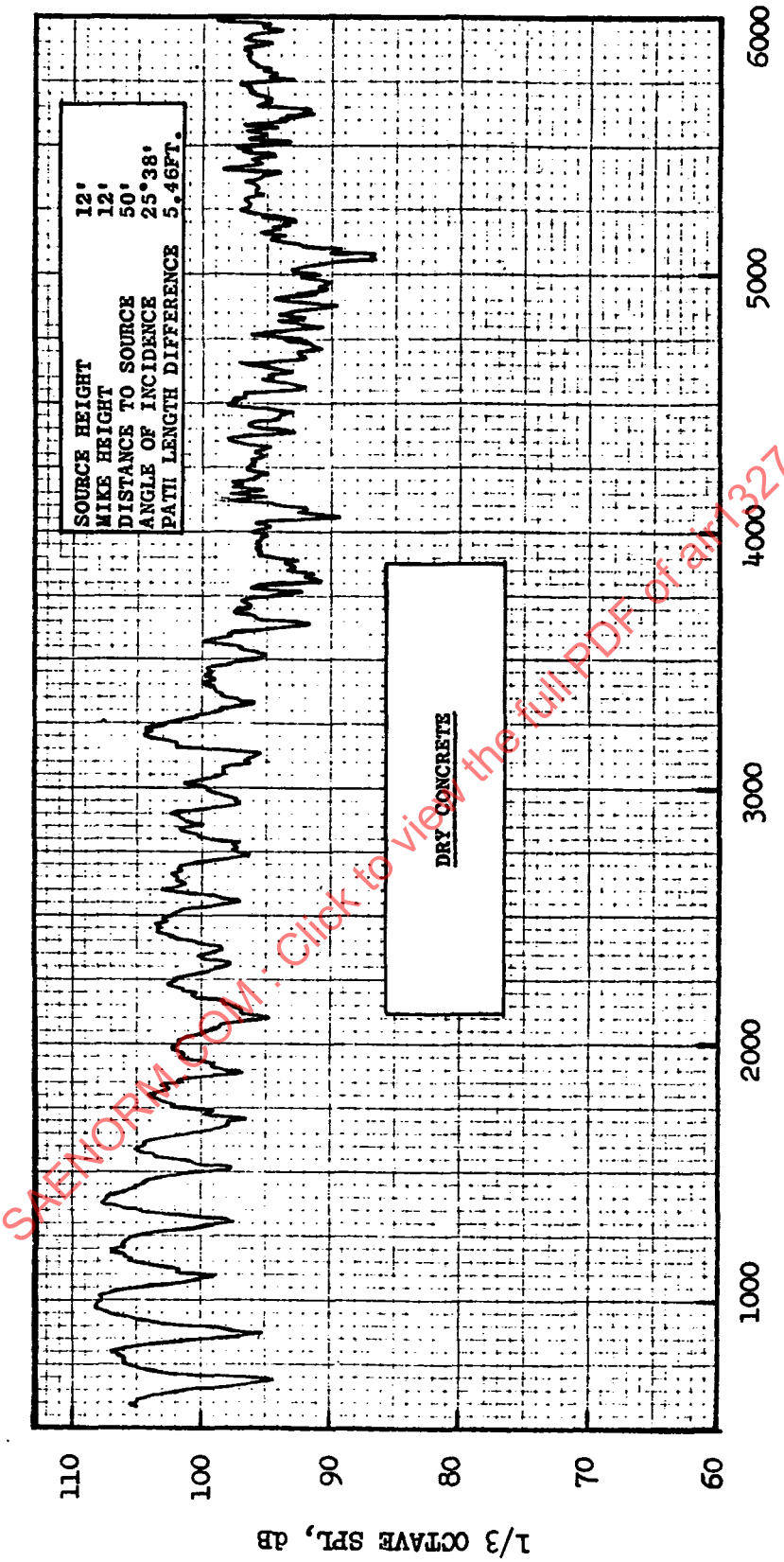


FIGURE (5-4) GROUND REFLECTION TESTS - DRY CONCRETE